References

1 Kidani Y, Noji M, Tashiro T. Antitumor activity of platinum(II) complexes of 1,2-diamino-cyclohexane isomers. *Gann* 1980; **71**: 637–43.
2 Mathe G, Kidani Y, Noji M, Maral R, Bourut C, Chenu E. Antitumor activity of l-OHP in mice. *Cancer Lett* 1985; **27**: 135–43.
3 Pendyala L, Creaven PJ. In vitro cytotoxicity, protein binding, red blood cell partitioning, and biotransformation of oxaliplatin. *Cancer Res* 1993; **53**: 5970–6.
4 Saltz LB, Cox JV, Blanke C *et al.* Irinotecan plus fluorouracil and leucovorin for metastatic colorectal cancer. Irinotecan Study Group. *N Engl J Med* 2000; **343**: 905–14.
5 Goldberg RM, Sargent DJ, Morton RF *et al.* A randomized controlled trial of fluorouracil plus leucovorin, irinotecan, and oxaliplatin combinations in patients with previously untreated metastatic colorectal cancer. *J Clin Oncol* 2004; **22**: 23–30.
6 Matsumura Y, Maeda H. A new concept for macromolecular therapeutics in cancer chemotherapy: mechanism of tumoritropic accumulation of proteins and the antitumor agent smancs. *Cancer Res* 1986; **46**: 6387–92.
7 Suzuki R, Takizawa T, Kuwata Y *et al.* Effective anti-tumor activity of oxaliplatin encapsulated in transferrin-PEG-liposome. *Int J Pharm* 2008; **346**: 143–50.
8 Abu Lila AS, Kizuki S, Doi Y, Suzuki T, Ishida T, Kiwada H. Oxaliplatin encapsulated in PEG-coated cationic liposomes induces significant tumor growth suppression via a dual-targeting approach in a murine solid tumor model. *J Control Release* 2009; **137**: 8–14.
9 Abu-Lila AS, Suzuki T, Doi Y, Ishida T, Kiwada H. Oxaliplatin targeting to angiogenic vessels by PEGylated cationic liposomes suppresses the angiogenesis in a dorsal air sac mouse model. *J Control Release* 2009; **134**: 18–25.
10 Kano MR, Bae Y, Iwata C *et al.* Improvement of cancer-targeting therapy, using nanocarriers for intractable solid tumors by inhibition of TGF-beta signaling. *Proc Natl Acad Sci USA* 2007; **104**: 3460–5.
11 ten Hagen TL, van Der Veen AH, Nooijen PT, van Tiel ST, Seynhaeve AL, Eggermont AM. Low-dose tumor necrosis factor-alpha augments antitumor activity of stealth liposomal doxorubicin (DOXIL) in soft tissue sarcoma-bearing rats. *Int J Cancer* 2000; **87**: 829–37.
12 Seynhaeve AL, Hoving S, Schipper D *et al.* Tumor necrosis factor alpha mediates homogeneous distribution of liposomes in murine melanoma that contributes to a better tumor response. *Cancer Res* 2007; **67**: 9455–62.
13 Kerbel RS, Kamen BA. The anti-angiogenic basis of metronomic chemotherapy. *Nat Rev Cancer* 2004; **4**: 423–36.
14 Laquente B, Vinals F, Germa JR. Metronomic chemotherapy: an antiangiogenic scheduling. *Clin Transl Oncol* 2007; **9**: 93–8.
15 Shiraga E, Barichello JM, Ishida T, Kiwada H. A metronomic schedule of cyclophosphamide combined with PEGylated liposomal doxorubicin has a highly antitumor effect in an experimental pulmonary metastatic mouse model. *Int J Pharm* 2008; **353**: 65–73.
16 Ishida T, Shiraga E, Kiwada H. Synergistic antitumor activity of metronomic dosing of cyclophosphamide in combination with doxorubicin-containing PEGylated liposomes in a murine solid tumor model. *J Control Release* 2009; **134**: 194–200.
17 Shirasaka T, Nakano K, Takechi T *et al.* Antitumor activity of 1 M tegafur-0.4 M 5-chloro-2,4-dihydroxypyridine-1 M potassium oxonate (S-1) against human colon carcinoma orthotopically implanted into nude rats. *Cancer Res* 1996; **56**: 2602–6.
18 Sakata Y, Ohtsu A, Horikoshi N, Sugimachi K, Mitachi Y, Taguchi T. Late phase II study of novel oral fluoropyrimidine anticancer drug S-1 (1 M tegafur-0.4 M gimestat-1 M otastat potassium) in advanced gastric cancer patients. *Eur J Cancer* 1998; **34**: 1715–20.
19 Sakuramoto S, Sasako M, Yamaguchi T *et al.* Adjuvant chemotherapy for gastric cancer with S-1, an oral fluoropyrimidine. *N Engl J Med* 2007; **357**: 1810–20.
20 Bartlett GR. Colorimetric assay methods for free and phosphorylated glyceric acids. *J Biol Chem* 1959; **234**: 469–71.
21 Cabral H, Nishiyama N, Kataoka K. Optimization of (1,2-diamino-cyclohexane)platinum (II)- loaded polymeric micelles directed to improved tumor targeting and enhanced antitumor activity. *J Control Release* 2007; **121**: 146–55.
22 Harashima H, Yamane C, Kume Y, Kiwada H. Kinetic analysis of AUC-dependent saturable clearance of liposomes: mathematical description of AUC dependency. *J Pharmacokinet Biopharm* 1993; **21**: 299–08.
23 Yamada Y, Tahara M, Miya T *et al.* Phase I/II study of oxaliplatin with oral S-1 as first-line therapy for patients with metastatic colorectal cancer. *Br J Cancer* 2008; **98**: 1034–8.
24 Grothey A. Oxaliplatin-safety profile: neurotoxicity. *Semin Oncol* 2003; **30**: 5–13.
25 Pietrangeli A, Leandri M, Terzoli E, Jandolo B, Garufi C. Persistence of high-dose oxaliplatin-induced neuropathy at long-term follow-up. *Eur Neurol* 2006; **56**: 13–6.
26 Lu D, Wientjes MG, Lu Z, Au JL. Tumor priming enhances delivery and efficacy of nanomedicines. *J Pharmacol Exp Ther* 2007; **322**: 80–8.
27 Ooyama A, Oka T, Zhao HY, Yamamoto M, Akiyama S, Fukushima M. Anti-angiogenic effect of 5-Fluorouracil-based drugs against human colon cancer xenografts. *Cancer Lett* 2008; **267**: 26–36.
28 Nagano S, Perentes JY, Jain RK, Boucher Y. Cancer cell death enhances the penetration and efficacy of oncolytic herpes simplex virus in tumors. *Cancer Res* 2008; **68**: 3795–802.
29 Daemen T, Regts J, Meesters M, ten Kate MT, Bakker-Woudenberg IA, Scherphof GL. Toxicity of doxorubicin entrapped within long-circulating liposomes. *J Control Release* 1997; **44**: 1–9.
30 Phillips NC. Kupffer cells and liver metastasis. Optimization and limitation of activation of tumoricidal activity. *Cancer Metastasis Rev* 1989; **8**: 231–52.
31 Iyer AK, Khaled G, Fang J, Maeda H. Exploiting the enhanced permeability and retention effect for tumor targeting. *Drug Discov Today* 2006; **11**: 812–8.

Journal of Controlled Release 142 (2010) 160–166

Contents lists available at ScienceDirect

Journal of Controlled Release

journal homepage: www.elsevier.com/locate/jconrel

CpG motifs in pDNA-sequences increase anti-PEG IgM production induced by PEG-coated pDNA-lipoplexes

Tatsuaki Tagami [a], Kazuya Nakamura [a], Taro Shimizu [a], Naoshi Yamazaki [b], Tatsuhiro Ishida [a], Hiroshi Kiwada [a,*]

[a] Department of Pharmacokinetics and Biopharmaceutics, Subdivision of Biopharmaceutical Sciences, Institute of Health Biosciences, The University of Tokushima, 1-78-1, Sho-machi, Tokushima 770-8505, Japan

[b] Department of Medicinal Biochemistry, Subdivision of Biopharmaceutical Sciences, Institute of Health Biosciences, The University of Tokushima, 1-78-1, Sho-machi, Tokushima 770-8505, Japan

ARTICLE INFO

Article history:
Received 6 July 2009
Accepted 14 October 2009
Available online 20 October 2009

Keywords:
Accelerated blood clearance (ABC) phenomenon
Polyethylene glycol (PEG)
Anti-PEG IgM
PEG-coated pDNA-lipoplex
CpG motifs

ABSTRACT

Gene therapy is largely dependent on the development of efficient delivery vehicles. To prolong their circulating time, PEGylation of the surface of a delivery vehicle is frequently applied. However, we have reported previously that anti-PEG IgM produced by intravenous injection of PEG-coated liposome is responsible for enhanced clearance of second dose PEG-coated liposomes, which is known as the "accelerated blood clearance (ABC) phenomenon." A similar phenomenon has been observed with PEG-coated pDNA-lipoplexes (PDCLs) upon their repeated injection. But the effect of the sequence of pDNA in PDCLs on inducing the ABC phenomenon has not been thoroughly investigated. Here, we focus on CpG motifs in pDNA, which are known to have a potent immune-stimulatory activity. PDCLs with non-CpG pDNA (PNDCL) diminished the anti-PEG IgM response, resulting in significant accumulation of a second dose in tumor tissue, comparable to that of a single injection, but not in enhanced accumulation in liver. In addition, PDCL induced proliferation of IgM^+ splenic cells including B cells. These results suggest that the CpG motif is a major cause of the induction of the ABC phenomenon when PDCLs are repeatedly injected. Immunogenicity is a relevant point of concern for non-viral delivery systems. Our results indicate that the use of non-CpG pDNA may allow meaningful repeated dosing of pDNA formulations without the induction of a strong immune reaction and thus may have important implications for therapeutic use of liposomal formulations of nucleic acids.

1. Introduction

Gene therapy has been proposed as a promising strategy for treating genetic and acquired diseases, but convincing therapeutic results have been limited thus far, predominantly because of a lack of sufficiently efficient and safe delivery system [1,2]. Although viral vectors are highly efficient, there are justified concerns about their safety related to immunogenicity and random incorporation of the delivered gene into the host genome. On the other hand, non-viral vectors, despite their relatively low transfer efficiency, are attractive alternatives to viral vectors because of their safety, versatility and ease of preparation and scaling-up.

Cationic liposomes present one of the most useful non-viral vector systems [3]. pDNA/cationic liposome complexes (pDNA-lipoplexes) can bind efficiently to the cell surface via charge–charge interactions, followed by internalization into the cells and subsequent gene expression *in vitro*. However, therapeutic success of pDNA-lipoplexes in the clinical situation, requiring for example systemic delivery, is jeopardized due to short blood circulation times. Surface modification of pDNA-lipoplexes with polyethylene glycol (PEG)-conjugated lipid (PEGylation) is frequently applied to prolong circulation time of lipoplexes [4]. It is believed that the PEG on the liposomal surface attracts a water shell, resulting in the reduced adsorption of opsonins and thus the recognition of the lipoplexes by the cells of the mononuclear phagocyte system (MPS) [5,6]. The PEG-coated pDNA-lipoplexes (PDCLs) thus obtained possess long circulation properties, and therefore can accumulate efficiently in solid tumors [7] because of the enhanced vascular permeability and retention effect in growing tumors [8].

However, we and others have reported that an intravenous injection of PEG-coated liposomes causes a second dose of material, injected a few days later, to lack the long-circulating characteristics of the first dose and to extensively accumulate in the liver [9,10]. This phenomenon is known as the "accelerated blood clearance (ABC) phenomenon." Based on earlier results [11,12], we have proposed the following tentative mechanism of this phenomenon: anti-PEG IgM,

* Corresponding author. Tel.: +81 88 633 7259; fax: +81 88 633 7260.
E-mail address: hkiwada@ph.tokushima-u.ac.jp (H. Kiwada).

0168-3659/$ – see front matter © 2009 Elsevier B.V. All rights reserved.
doi:10.1016/j.jconrel.2009.10.017

produced in the spleen in response to a first dose, selectively binds to the PEG of the second dose of liposomes injected several days later and subsequently activates the complement system. This, in turn, leads to opsonization of the second dose of liposomes by C3 fragments and, as a consequence, to enhanced uptake of the liposomes by the Kupffer cells in the liver.

The ABC phenomenon involving anti-PEG IgM production is an important factor to be considered in designing an efficient delivery system of genes or nucleic acids. Judge et al. [7] have recently reported that PEG-coated lipid nano-particles encapsulating pDNA greatly enhance anti-PEG IgM production when compared with PEG-coated nano-particles without encapsulated pDNA, and that, as a consequence, gene expression relating to pDNA in tumor tissue was strongly diminished following its second injection. However, the mechanism underlying the enhancing effect of pDNA on anti-PEG IgM response and the accelerated blood clearance of the second dose of PEG-coated lipid nano-particles encapsulating pDNA has not been elucidated yet. Here, we focus on CpG motifs in the pDNA-sequence, which can activate the toll-like receptor 9 (TLR9) signaling pathway in immune competent cells and induce the production of a variety of inflammatory cytokines and interferons [13]. In addition, CpG motifs have a strong adjuvant effect which contributes to the increased immunogenicity [14]. In view of these considerations it would not be surprising if the presence of CpG motifs in pDNA formulations would act as a potent stimulator of the IgM response. In the present study, we investigated the effect of CpG motifs in pDNA-sequence on anti-PEG IgM production induced by PEG-coated pDNA-lipoplexes and the contribution of splenic B cells to the anti-PEG IgM responses caused by PEG-coated pDNA-lipoplexes.

2. Materials and methods

2.1. Materials

2-distearoyl-*sn*-glycero-3-phosphoethanolamine-*n*-[methoxy (polyethylene glycol)-2000] ($mPEG_{2000}$-DSPE), 1-palmitoyl-2-oleoyl-*sn*-glycero-3-phosphocholine (POPC) and dioleoylphosphatidylethanolamine (DOPE) were generously donated by NOF (Tokyo, Japan). A cationic lipid, O,O′-ditetradecanoyl-N-(α-trimethyl ammonio acetyl) diethanolamine chloride (DC-6-14) was purchased from Sogo Pharmaceutical (Tokyo, Japan). Cholesterol (CHOL) was of analytical grade (Wako Pure Chemical, Osaka, Japan). All lipids were used without further purification. ^{3}H-Cholesterylhexadecyl ether (^{3}H-CHE) was purchased from PerkinElmer Life Science (MA, USA). All other reagents were of analytical grade.

2.2. Preparation of pDNA

pEGFP-N1 which contains CpG motifs (4733 bp, 321 CpG points (13.56%)) was purchased from Clontech (CA, USA). pCpG-mcs (3066 bp) which lacks CpG motifs was purchased from Invivogen (CA, USA). pEGFP-N1 and pCpG-mcs were amplified in E. coli strain DH5α and GT115, isolated by using EndoFree Plasmid Maxi Kit (Qiagen, Hilden, Germany). The level of endotoxin in the DNA preparation was always <0.1 endotoxin unit/μg DNA as measured by the Limulus amoebocyte lysate assay (BioWhittaker, MO, USA).

2.3. Animals and cells

Male Std-ddY mice aged 4–5 weeks (20–25 g), male BALB/cCr Slc mice aged 4–5 weeks (20–25 g) and male BALB/c Slc-nu/nu mice aged 5–6 weeks (20–25 g) were purchased from Japan SLC (Shizuoka, Japan). Mice were maintained under pathogen-free conditions. All animal experiments were evaluated and approved by the Animal and Ethics Review Committee of the University of Tokushima.

Mouse sarcoma, sarcoma 180 (S-180) cells were injected intraperitoneally and maintained in the peritoneum of ddY mice. Mice were sacrificed at 2 weeks after intraperitoneal inoculation of S-180 cells and the ascitic fluid containing S-180 cells was collected. Cells were washed 3 times by phosphate buffered saline (PBS), and the prepared cell suspension was used for subsequent experiments.

2.4. Preparation of cationic liposomes

Cationic liposomes were composed of DC-6-14:POPC:CHOL:DOPE (10:30:30:30, molar ratio). Liposomes were prepared as previously described [15]. Briefly, the lipids were dissolved in chloroform, and after evaporation of the organic solvent, the resulting lipid film was hydrated in 9% sucrose to produce multilamellar vesicles (MLVs). The MLVs were sized by repeated extrusion thorough polycarbonate membrane filters (Nucleopore, CA, USA) with consecutive pore sizes of 400, 200 and 100 nm. The mean diameters and zeta potentials of the resulting liposomes were determined using a NICOMP 370 HPL submicron particle analyzer (Particle Sizing System, CA, USA). The mean diameter and zeta potential for cationic liposomes were 93.4 nm and +20.4 mV ($n=3$), respectively. The lipid concentration of the liposomes was determined by using a Cholesterol E-test Wako kit (Wako Pure Chemical, Osaka, Japan) and approximately 25 mM.

2.5. Preparation of PEG-coated pDNA-lipoplexes (PDCLs) and PEG-coated "empty" cationic liposomes (PCL)

For the formulation of pDNA-lipoplexes, pDNA (10 μg) and cationic liposomes (1 μmol, phospholipids) were mixed at 3.82 (+/−) charge ratio and incubated for 20 min at room temperature. For PEGylation, a post-insertion technique was employed [16,39]. Briefly, $mPEG_{2000}$-DSPE (5 mol% of total lipid) in 9% sucrose solution was added into either pDNA-lipoplex or cationic liposome solution. The mixture was vortexing and gently shaking for 1 h at 37 °C. Under the condition, almost 100% of $mPEG_{2000}$-DSPE added could be incorporated into preformed pDNA-lipoplexes [16]. The mean diameter was 315.3 nm for PEG-coated pDNA-lipoplexes (PDCLs), 309.9 nm for PEG-coated non-CpG pDNA-lipoplexes (PNDCL) and 108.1 nm for PEG-coated cationic liposomes (PCL) ($n=3$). The mean zeta potential was +14.5 mV for PDCLs, +13.1 mV for PNDCL and +20.5 mV for PCL ($n=3$). To determine the biodistribution of PEG-coated lipoplexes, cationic liposomes were labeled with a trace amount of ^{3}H-CHE (40 μCi/μmol of phospholipids) as a non-exchangeable lipid phase marker.

2.6. Biodistribution of single and second dose in tumor-bearing mice

S-180 cells (2×10^6 cells) were implanted subcutaneously in the dorsal skin of ddY mice. On day 2 after tumor inoculation, pretreatment was given. For the pretreatment, either PDCL, PNDCL (5 μmol phospholipids and 50 μg pDNA/mouse, approximately 125 μmol phospholipids and 1.25 mg pDNA per kg of body weight, respectively) or saline was intravenously administered into mice via the tail vein. On day 7 after tumor inoculation (5 days after the pretreatment) when the tumor had reached a diameter of 4–5 mm but no necrotic areas were apparent, radio (^{3}H-CHE)-labeled test dose (PDCL or PNDCL, 5 μmol phospholipids and 50 μg pDNA/mouse, respectively) was intravenously administered into the treated mice via the tail vein. At 24 h after the injection, the mice were sacrificed. Blood samples were withdrawn by heart puncture, and then tumor tissue as well as normal tissues including liver, kidney and lung were collected from the mice and weighed after withdrawing the blood samples. Radioactivities in blood and tissues were assayed as described previously [17].

2.7. Detection of anti-PEG IgM

A simple ELISA procedure as described previously [15] was employed to detect anti-PEG IgM in the serum. Briefly, 10 nmol of

$mPEG_{2000}$-DSPE in 50 μl ethanol was added to 96-well plates. Lipid-coated plates were allowed to air dry completely for 2 h. The plates were then blocked for 1 h with Tris-buffered saline containing 1% BSA and were subsequently washed three times. Diluted serum samples (1:100) (100 μl) were then applied in the wells, incubated for 1 h and washed. Horseradish peroxidase (HRP)-conjugated antibody (100 μl, 1 μg/ml, Goat anti-mouse IgM IgG-HRP conjugate; Bethyl Laboratories, TX, USA) was added to the wells. After 1 h incubation, the wells were washed three times. The coloration was initiated by adding 100 μl of *o*-phenylenediamine (1 mg/ml) (Sigma, MO, USA). After 15 min incubation, the reaction was stopped by adding 100 μl of 2 N H_2SO_4. The absorbance was measured at 490 nm using a microplate reader (Wallac1420 ARVOsx, PerkinElmer Life Science). All incubations were performed at room temperature.

2.8. In vivo B-cell proliferation (BrdU incorporation assay)

To assess *in vivo* B-cell proliferation, mice were given drinking water containing BrdU (Sigma) at 0.8 mg/ml, which was made fresh and changed daily. One day after the start of BrdU administration, either PDCL, PNDCL (5 μmol phospholipids and 50 μg pDNA/mouse) or PCL (5 μmol phospholipids/mouse) was intravenously administered via the tail vein. Two days later, the spleen was removed. Spleen single-cell suspensions were prepared as described previously [15]. Briefly, spleen slices were pressed through a Cell Strainer (100 μm, Becton Dickinson, NJ, USA) and cells were subsequently washed by PBS (pH 7.4, Nissui Pharmaceutical, Tokyo, Japan). Red blood cells were lysed by treatment with 5 mL of ammonium chloride lysis buffer (0.15 M NH_4Cl, 10 mM $KHCO_3$ 0.1 mM Na_4EDTA, pH 7.2) for 5 min on ice and subsequently washed.

IgM-expressing splenic B cells were stained with FITC-conjugated anti-mouse IgM (Goat anti-mouse IgM-FITC conjugate; American Qualex Antibodies, CA, USA) for 1 h at room temperature and subsequently washed. For staining BrdU incorporation, cells were fixed with 4% paraformaldehyde for 20 min at room temperature, permeabilized with 0.2% Triton-X for 15 min on ice and treated with 1 U of DNase/ml for 1 h at 37 °C and subsequently washed for each procedure. Cells were then incubated with Phycoerythrin (PE)-conjugated anti-mouse BrdU (Goat anti-mouse BrdU-PE conjugate; Santa Cruz Biotechnology, CA, USA) for 1 h at room temperature and subsequently washed. Cells were analyzed by using a flow cytometer, Guava EasyCyte Mini (Guava Technologies, CA, USA).

2.9. Statistical analysis

All values are expressed as the mean ± S.D. Statistical analysis was performed with a two-tailed unpaired Student's *t* test using GraphPad InStat software (GraphPad Software, CA, USA). The level of significance was set at $p < 0.05$.

3. Results

3.1. Anti-PEG IgM production induced by a single injection of either PCL, PDCL or PNDCL

We determined the effect of the presence of pDNA in the PEG-coated lipoplex on anti-PEG IgM production. Anti-PEG IgM production was assessed on day 5 after a single injection of either PEG-coated "empty" cationic liposome (PCL) or PEG-coated pDNA-lipoplexes (PDCLs), by which time the ABC phenomenon is markedly manifest [18]. We confirmed that a low-dose single injection of PCL caused a significant induction of anti-PEG IgM production (Fig. 1). Consistent with our earlier observations [19], the level of induction was reversely related to the dose of PCL: the higher dose the lower the induction. PDCLs also induced substantial production of anti-PEG IgM at low dose, but here no decline in response was observed upon increasing

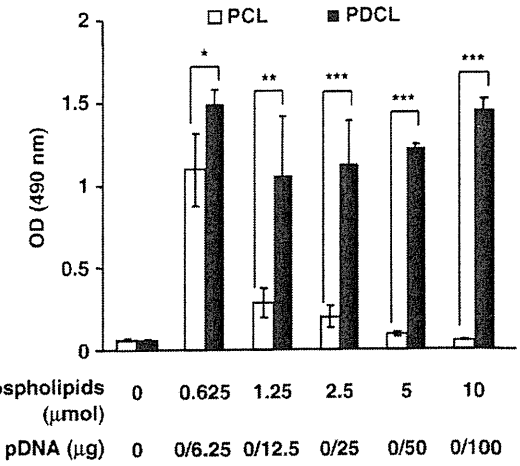

Fig. 1. Anti-PEG IgM production induced by a single injection of either PCL or PDCL. PCLs or PDCLs were intravenously injected at the indicated doses. Five days later, blood was withdrawn from each treated mouse and serum was collected. The sera collected from the naïve mice were used as controls (dose 0). PCL did not contain pDNA. Anti-PEG IgM was detected with ELISA as described in Materials and methods. Each value represents the mean ± SD ($n = 4$). $^*p < 0.05$, $^{**}p < 0.01$, $^{***}p < 0.005$.

the dose. Apparently, pDNA in the lipoplexes strongly stimulated the immune system to produce anti-PEG IgM.

Fig. 2 presents the results of experiments in which we studied the effect of CpG motifs in the pDNA entrapped in the PCL, on anti-PEG IgM production. On day 5 after a single injection of either PDCL or PEG-coated non-CpG pDNA-lipoplex (PNDCL), anti-PEG IgM in serum was determined. Clearly, PNDCL with non-CpG pDNA caused a much lower the anti-PEG IgM response than PDCL with CpG-containing pDNA. It is well known that CpG motifs in pDNA are a potent immune stimulator [14]. Hence, it is likely that the CpG motifs in pDNA were a major cause of the enhanced anti-PEG IgM production at the higher dose of PDCLs, as presented in Fig. 1.

3.2. Effect of prior dosing on biodistribution of test doses of PDCL or PNDCL

The biodistribution of radio-labeled test doses of PDCL or PNDCL was investigated with or without pre-dosing 24 h after injection. As shown in Fig. 3, without pre-dosing there were no significant differences between PDCL and PNDCL in the fractions of injected

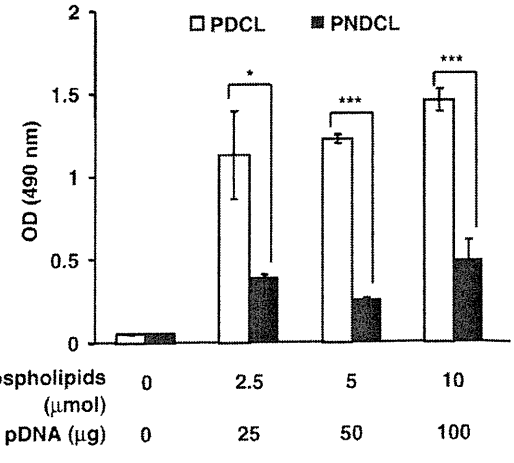

Fig. 2. Effect of CpG motifs in pDNA on anti-PEG IgM production induced by PEG-coated pDNA-lipoplexes. Experimental conditions were identical to those in Fig. 1 except that PDCLs or PNDCLs were injected.

dose remaining in blood and accumulating in all organs including tumor. This indicates that the CpG motif in pDNA by itself does not affect the biodistribution of PEG-coated lipoplexes in mice.

After pre-dosing, however, significant differences were observed between biodistribution of the second test doses of the two types of particle. Again, tumor-bearing mice received a radio-labeled test dose of either PDCL or PNDCL, but now after first having received a pre-dose of the same particles 5 days earlier. Test-dose radioactivity in blood, major organs and implanted tumor was determined 24 h after injection. After pre-dosing, blood clearance and biodistribution of the second PDCL dose were markedly altered (Fig. 3). The amount remaining in blood was less than half of that found without pre-dosing, while accumulation of PDCLs in liver and spleen was significantly enhanced and that in tumor substantially reduced. A prior injection of PNDCL, on the other hand, did not at all affect the biodistribution of a second test PNDCL dose. These results suggest that the CpG motifs in the pDNA in PDCLs, are the major cause of the enhanced blood clearance of test-dose particles, resulting in substantially reduced accumulation in tumor tissue.

3.3. Anti-PEG IgM production in T-cell-deficient (nude) mice

We recently reported that an intravenous injection of PEG-coated "empty" liposomes or PEG-coated siRNA-lipoplex caused anti-PEG IgM production in a T-cell-independent manner [15,18]. To study the contribution of T cells to anti-PEG IgM production, T-cell-deficient (nude) mice received either PCL, PDCL or PNDCL. As shown in Fig. 4, anti-PEG IgM production was detected in all pretreated nude mice. This indicates that T cells do not play an important role in the anti-PEG IgM production. Interestingly, anti-PEG IgM production induced by PCL (both doses) or PNDCL (only higher dose) was significantly enhanced in nude mice compared to in naïve mice. It would appear that T cells in naïve mice rather attenuate the production of anti-PEG IgM in a dose-dependent manner.

3.4. Proliferation of IgM-expressing splenic B cells in vivo

In our earlier studies, we showed that spleen plays an important role in the production of anti-PEG IgM [11,18]. Because it is well known that B cells secrete IgM while extensively proliferating in spleen [20–22], we assumed that CpG motifs in pDNA might act as "B-cell mitogen," resulting in enhanced proliferation of splenic B cells.

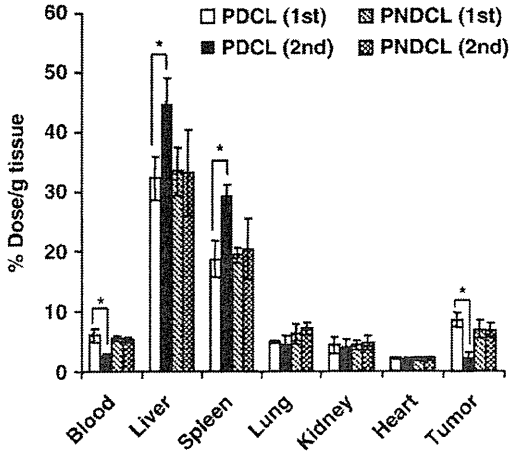

Fig. 3. Effect of prior dose on biodistribution of test doses of PDCL or PNDCL. At day 5 after the pretreatment with either PDCLs or PNDCLs (5 μmol phospholipids and 50 μg pDNA/mouse), ^{3}H-CHE labeled PDCLs or PNDCLs (5 μmol phospholipids and 50 μg pDNA/mouse) were intravenously injected. At 24 h after injection, ^{3}H activity in each tissue and blood was determined as described in Materials and methods. "1st" means without pretreatment. "2nd" means with pretreatment. Each value represents the mean ± SD ($n = 4$). * $p < 0.05$.

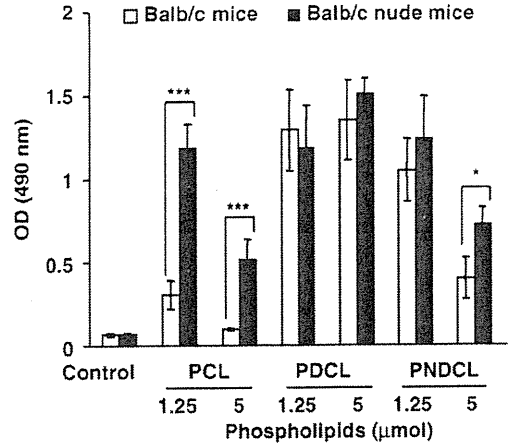

Fig. 4. Anti-PEG IgM production in T-cell-deficient (nude) mice. Either PCL, PDCL or PNDCL was intravenously injected into (A) BALB/c mice or (B) BALB/c nude mice. Five days later, blood was withdrawn from each mice and serum was collected. The sera collected from the naïve (non-treated) mice were used as controls. Anti-PEG IgM was detected with ELISA as described in Materials and methods. Each value represents the mean ± SD ($n = 4$). *$p < 0.05$, ***$p < 0.005$.

Therefore we determined BrdU incorporation and IgM expression in splenic cells by means of double immunofluorescent staining and flow-cytometric analysis at day 2 after a single injection of either PCL, PDCL or PNDCL (5 μmol phospholipids/mouse) (Fig. 5). The treatments with PCL, PDCL and PNDCL induced BrdU incorporation by IgM^{+} splenic cells, as compared to saline treatment. As expected, among these treatments, PDCLs showed the highest BrdU incorporation by IgM^{+} splenic cells, indicating that PDCLs did trigger proliferation of IgM-expressing splenic B cells. It appeared that CpG motifs in pDNA of PDCLs play a role as "B-cell mitogen," resulting in proliferation of splenic IgM-expressing cells, presumably splenic B cells.

4. Discussion

The use of non-viral vectors for gene therapy has many advantages over viral vectors such as safety, productivity and simplicity [1,2]. However, for *in vivo* use, repeated injections of such vectors will be required to compensate for their low transfection efficiency relative to viral vectors [23,24]. PEG-coated non-viral vectors have substantial advantages in prolonging blood circulation of drugs, including nucleic acids such as pDNA, oligodeoxynucleotide (ODN) or small interference RNA (siRNA). However, we have reported earlier that an intravenous injection of PEG-coated "empty" liposome causes a second dose of PEG-coated liposome, injected a few days later, to lose its long-circulating characteristics and to accumulate extensively in the liver [10] as a result of induction of anti-PEG IgM production by the first dose of PEG-coated "empty" liposomes [12,15]. This phenomenon is known as the "ABC phenomenon" [9]. Judge et al. recently reported that PEG-coated lipid nano-particles encapsulating pDNA cause an acute loss of prolonged blood circulation of a second dose due to enhanced anti-PEG IgM production [7]. However, the influence of the sequence of the encapsulated pDNA in the PEG-coated lipoplexes, namely the occurrence of CpG motifs, on the anti-PEG IgM response has not been thoroughly investigated yet.

In the present study, we showed that encapsulation of pDNA containing CpG motifs in PEG-coated cationic liposomes further facilitated the induction of anti-PEG IgM production (Fig. 1) while the use of non-CpG pDNA instead of pDNA with CpG motifs rather diminished the anti-PEG IgM production (Fig. 2). These findings clearly indicate that CpG motifs in pDNA play a key role in the induction of anti-PEG IgM production by intravenous injection of PEG-coated pDNA-lipoplexes and that the encapsulation of immune-

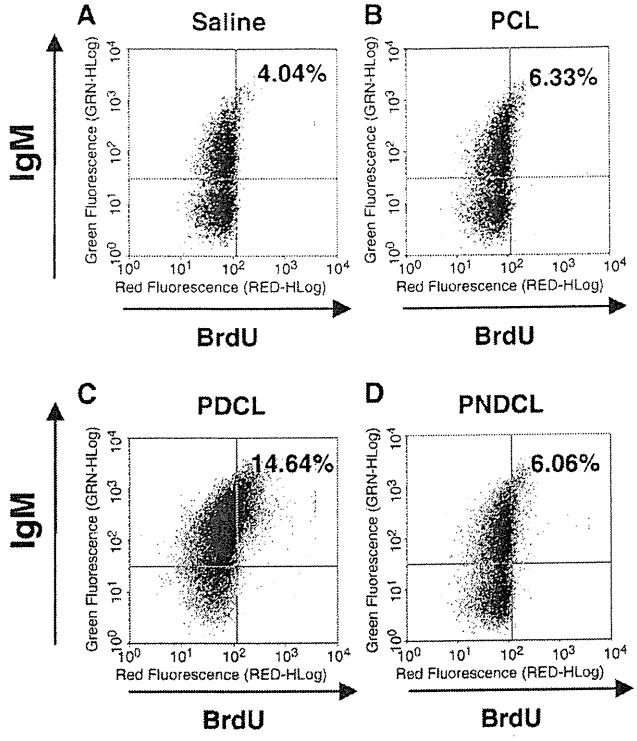

Fig. 5. Differentiation of IgM^+ splenic cells *in vivo*. The mice were treated with (A) saline as controls, (B) PCL, (C) PDCL, or (D) PNDCL (5 μmol phospholipids and 50 μg pDNA/mouse, except for PCL (lipid only)). The mice were given drinking water containing BrdU continually for 3 days to label proliferating cells. Two color staining of spleen cell suspensions for flow cytometry identified IgM^+ splenic cells incorporating BrdU. Plots are representative of splenic cells from three mice in each group. Values in the upper right quadrant represent percentage IgM^+ $BrdU^+$ splenocytes.

stimulatory pDNA within PEG-coated cationic liposome is sufficient to render the PEGylated vehicles even more immunogenic. It should not come as a surprise that the presence of encapsulated pDNA in PEG-coated cationic liposomes could potentially induce the anti-PEG IgM response, because CpG motifs in bacterial DNA and some antisense ODN have been shown to have strong mitogenic properties *in vitro*, resulting in lymphocyte proliferation and IgM production [25].

As shown in Figs. 1 and 2, only PDCLs caused anti-PEG IgM production when it was given at a dose of 5 μmol phospholipids/mouse. In addition, the intravenous injection of PDCLs resulted in the induction of the ABC phenomenon. This suggests that CpG-motif-induced anti-PEG IgM production was causing the ABC phenomenon against the second PDCL dose. This would lead to the conclusion that CpG motifs also play an important role in the induction of the ABC phenomenon as a consequence of increased anti-PEG IgM production.

Since pDNA can act as a polyclonal B-cell activator [25], we examined the B-cell proliferation response to PEG-coated pDNA-lipoplexes *in vivo* to determine if the production of anti-PEG IgM is part of a generalized polyclonal antibody response. Regardless of pDNA encapsulation, all PEG-coated cationic liposome formulations increased the proportion of IgM^+ splenic cells when they were injected at a dose of 5 μmol phospholipids/mouse (Fig. 5), although the numbers of cells were very small. This indicates that the generation of anti-PEG IgM reflects the selective activation and differentiation of a small subset of splenic IgM^+ cells, presumably B cells, as Judge et al. have shown earlier [7]. Interestingly, of the three formulations tested, PDCLs, which contains pDNA with CpG motifs, induced the most extensive differentiation of IgM^+ splenic cells (B cells) (Fig. 5). It appeared that CpG motifs in pDNA selectively activated splenic B cells presumably via a stimulatory pathway such as TLR9 [26], resulting in further enhanced induction of anti-PEG IgM following intravenous injection of PDCLs. It is well known that TLR9 play a critical role in innate immunity through the production of inflammatory cytokines such as IL-6, IL-12 and TNF-α and interferons [25,26], and that IL-6 or INF-γ is strongly related with the promotion of IgM production [39]. Therefore, the detection of inflammatory cytokines or interferons following intravenous injection of PDCLs may give more critical information regarding how CpG motif in the pDNA acts as an adjuvant to activate IgM^+ B cells.

We recently reported that higher doses of "empty" PEG-coated liposome resulted in the reduction of anti-PEG IgM [18,19] presumably by inducing apoptosis of IgM^+ B cells in spleen. In this study, PDCL induced anti-PEG IgM production at higher dose (Fig. 1) as a result of IgM^+ B-cell differentiation in spleen (Fig. 5), while "empty" PCL reduced anti-PEG IgM production at higher dose (Fig. 1) as observed previously [18,19]. These demonstrate that the B-cell mitogen activity of the CpG motif in the PDCLs might be over the apoptotic activity of "empty" PEG-coated liposome at the higher doses.

PEG-lipid itself is considered a weak antigen [27] so that PEG-lipid has been widely used in the pharmaceutical industry to improve the pharmacokinetics and reduce the immunogenicity of various therapeutic agents [28]. However, our earlier results clearly indicated that PEG-lipids display immunogenicity when incorporated in liposomes without any payloads [29]. In this study, all PEG-coated cationic liposome formulations produced anti-PEG IgM in a T-cell-independent manner (Fig. 4), which is consistent with our earlier results with PEG-coated "empty" liposomes and PEG-coated siRNA-lipoplexes [12,15,18] and with an observation of Semple et al. on ODN [30]. Hence, it is likely that PEG-lipid in the liposomal membrane functions as a T-cell-independent antigen, although the detailed mechanism has not been elucidated yet. In addition, our current results clearly indicate that the T-cell-independent IgM response against PEG-lipid is further facilitated in the presence of encapsulated pDNA containing CpG motifs. As far as we know, this is the first report showing that the presence of liposome encapsulated pDNA functions as an adjuvant for the generation of immune responses to a weak T-cell-independent antigen, PEG-lipid, in a sequence-dependent manner.

Following intravenous injections of PCL (without pDNA) at 1.25 and 5 μmol phospholipids/mouse and PNDCL (containing non-CpG pDNA) at 5 μmol phospholipids/mouse, the anti-PEG IgM response was rather substantial in immunodeficient athymic (nude) mice (Fig. 4), which are preferentially employed to distinguish T-cell dependency of the immune reaction [31]. This may suggest that T cells in naïve mice inhibit anti-PEG IgM production induced by PEG-coated cationic liposomes or lipoplexes in a dose-dependent manner. Regulatory T cells have been shown to play an important role in the regulation of a variety of immune responses. Interleukin 10 (IL-10), an immunomodulatory cytokine predominantly produced by monocytes/macrophages and T cells, suppresses or induces the activation of immune system [32]. Pecanha et al. reported that IL-10 inhibits IgM secretion of B cells induced by T-cell-independent antigens *in vitro* [33]. Therefore, IL-10 secreted from regulatory T cells might lead a tolerance towards the anti-PEG IgM response of B cells in naïve mice [34], but not in T-cell-deficient (nude) mice, when relatively high doses were given (Fig. 4). However, the factors controlling T-cell IL-10 production are complex and still not completely understood. Hence, the effect of T-cell IL-10 on the anti-IgM production induced by PEG-coated liposomes still needs to be elucidated.

The ability to abrogate the immunogenicity of PEG-coated lipoplexes containing encapsulated nucleic acid drugs such as pDNA, siRNA and ODN by simple modification of their lipid composition without significantly compromising *in vivo* performance has important implications for the design and clinical development of promising delivery systems. Judge et al. [7] recently proposed that the immunogenicity of PEG-coated liposomes containing pDNA can be greatly reduced by using alternative PEG-lipids that dissociate more readily from the lipid bilayer upon systemic administration. In this study, we demonstrated that the immunogenicity of PEG-coated cationic liposomes containing pDNA can be reduced by selecting less immunostimulatory pDNA such as CpG-free pDNA, instead of immunostimulatory pDNA, as payloads (Fig. 2). Consequently, second dose PEG-coated non-CpG pDNA-lipoplexes (PNDCL) accumulated in tumor to similar extents as the first PNDCL dose (Fig. 3). Non-CpG pDNAs generally achieve sustained gene expression compared to pDNA containing CpG motifs, which are easily methylated in the nucleus causing transcriptional gene silencing [35,36]. In addition, non-CpG pDNAs do not induce inflammatory cytokine production [35,37,38], because of their lack of CpG motifs, which activate the TLR9 signaling pathway in immune competent cells and thereby induce production of inflammatory cytokines or interferons. Accordingly, the use of CpG-free pDNA instead of pDNA containing CpG motifs may meet the safety requirements of nucleic acid delivery systems for repeated administration. Hence, the results of our study may show the way to an alternative approach to reduce immunogenicity of PEG-coated carrier systems for nucleic acid drugs, upon repeated administration, yielding an efficient therapeutic effect in gene therapy without severe carrier-induced side effects.

5. Conclusion

The present study shows that the presence of CpG motifs in pDNA is a major cause of enhanced anti-PEG IgM production induced by PEG-coated pDNA-lipoplexes. The use of less immunostimulatory pDNA, e.g. non-CpG pDNA, significantly diminished the anti-PEG IgM production, resulting in abrogation of the induction of the ABC phenomenon. Thus, PEG-coated cationic lipoplexes containing non-CpG pDNA (PNDCL) may achieve efficient gene expression in the tumor upon repeated injection. Our study may have significant implications for the use of PEG-coated pDNA-lipoplexes in gene therapy.

Abbreviations

ABC	accelerated blood clearance phenomenon
^{3}H-CHE	^{3}H-Cholesterylhexadecyl ether
CHOL	cholesterol
DC-6-14	O,O'-ditetradecanoyl-N-(alpha trimethyl ammonioacetyl) diethanolamine chloride
DOPE	dioleoylphospatidylethanolamine
IL-10	interleukin 10
MLVs	multilamellar vesicles
$mPEG_{2000}$-DSPE	1,2-distearoyl-sn-glycero-3-phosphoethanolamine-*n*-[methoxy (polyethyleneglycol)-2000]
MPS	mononuclear phagocyte system
ODN	oligodeoxynucleotide
PBS	phosphate buffered saline
PCL	PEG-coated cationic liposome
pDNA	plasmid DNA
PDCL	PEG-coated pDNA-lipoplex
PEG	polyethylene glycol
PNDCL	PEG-coated non-CpG pDNA-lipoplex
POPC	1-palmitoyl-2-oleoyl-*sn*-glycero-3-phosphocholine
siRNA	small interference RNA
TLR	toll-like receptor

Acknowledgements

We thank Dr. G.L. Scherphof for his helpful advice in writing the English manuscript. This work was supported in part by the Health and Labour Sciences Research Grants for Research on Advanced Medical Technology from the Ministry of Health, Labour and Welfare of Japan, and by a grant-in-aid for scientific research on priority areas of cancer, Ministry of Education, Culture, Sports and Technology, Japan (20015033).

References

[1] M. Morille, C. Passirani, A. Vonarbourg, A. Clavreul, J.P. Benoit, Progress in developing cationic vectors for non-viral systemic gene therapy against cancer, Biomaterials 29 (2008) 3477–3496.
[2] S.D. Li, L. Huang, Gene therapy progress and prospects: non-viral gene therapy by systemic delivery, Gene. Ther. 13 (2006) 1313–1319.
[3] P.L. Felgner, T.R. Gadek, M. Holm, R. Roman, H.W. Chan, M. Wenz, J.P. Northrop, G.M. Ringold, M. Danielsen, Lipofection: a highly efficient, lipid-mediated DNA-transfection procedure, Proc. Natl. Acad. Sci. U. S. A. 84 (1987) 7413–7417.
[4] W. Li, F.C. Szoka Jr., Lipid-based nanoparticles for nucleic acid delivery, Pharm. Res. 24 (2007) 438–449.
[5] D. Papahadjopoulos, T.M. Allen, A. Gabizon, E. Mayhew, K. Matthay, S.K. Huang, K.D. Lee, M.C. Woodle, D.D. Lasic, C. Redemann, et al., Sterically stabilized liposomes: improvements in pharmacokinetics and antitumor therapeutic efficacy, Proc. Natl. Acad. Sci. U. S. A. 88 (1991) 11,460–11,464.
[6] V.P. Torchilin, V.G. Omelyanenko, M.I. Papisov, A.A. Bogdanov Jr., V.S. Trubetskoy, J.N. Herron, C.A. Gentry, Poly(ethylene glycol) on the liposome surface: on the mechanism of polymer-coated liposome longevity, Biochim. Biophys. Acta. 1195 (1994) 11–20.
[7] A. Judge, K. McClintock, J.R. Phelps, I. Maclachlan, Hypersensitivity and loss of disease site targeting caused by antibody responses to PEGylated liposomes, Mol. Ther. 13 (2006) 328–337.
[8] Y. Matsumura, H. Maeda, A new concept for macromolecular therapeutics in cancer chemotherapy: mechanism of tumoritropic accumulation of proteins and the antitumor agent smancs, Cancer. Res. 46 (1986) 6387–6392.
[9] E.T. Dams, P. Laverman, W.J. Oyen, G. Storm, G.L. Scherphof, J.W. van Der Meer, F.H. Corstens, O.C. Boerman, Accelerated blood clearance and altered biodistribution of repeated injections of sterically stabilized liposomes, J. Pharmacol. Exp. Ther. 292 (2000) 1071–1079.
[10] T. Ishida, R. Maeda, M. Ichihara, K. Irimura, H. Kiwada, Accelerated clearance of PEGylated liposomes in rats after repeated injections, J. Control. Release. 88 (2003) 35–42.
[11] T. Ishida, M. Ichihara, X. Wang, H. Kiwada, Spleen plays an important role in the induction of accelerated blood clearance of PEGylated liposomes, J. Control. Release. 115 (2006) 243–250.
[12] T. Ishida, M. Ichihara, X. Wang, K. Yamamoto, J. Kimura, E. Majima, H. Kiwada, Injection of PEGylated liposomes in rats elicits PEG-specific IgM, which is responsible for rapid elimination of a second dose of PEGylated liposomes, J. Control. Release. 112 (2006) 15–25.
[13] D.M. Klinman, A.K. Yi, S.L. Beaucage, J. Conover, A.M. Krieg, CpG motifs present in bacteria DNA rapidly induce lymphocytes to secrete interleukin 6, interleukin 12, and interferon gamma, Proc. Natl. Acad. Sci. U. S. A. 93 (1996) 2879–2883.

[14] H. Hemmi, O. Takeuchi, T. Kawai, T. Kaisho, S. Sato, H. Sanjo, M. Matsumoto, K. Hoshino, H. Wagner, K. Takeda, S. Akira, A Toll-like receptor recognizes bacterial DNA, Nature 408 (2000) 740–745.
[15] T. Ishida, X. Wang, T. Shimizu, K. Nawata, H. Kiwada, PEGylated liposomes elicit an anti-PEG IgM response in a T cell-independent manner, J. Control. Release. 122 (2007) 349–355.
[16] T. Ishida, D.L. Iden, T.M. Allen, A combinatorial approach to producing sterically stabilized (Stealth) immunoliposomal drugs, FEBS. Lett. 460 (1999) 129–133.
[17] H. Harashima, C. Yamane, Y. Kume, H. Kiwada, Kinetic analysis of AUC-dependent saturable clearance of liposomes: mathematical description of AUC dependency, J. Pharmacokinet. Biopharm. 21 (1993) 299–308.
[18] T. Tagami, K. Nakamura, T. Shimizu, T. Ishida, H. Kiwada, Effect of siRNA in PEG-coated siRNA-lipoplex on anti-PEG IgM production, J. Control. Release. 137 (2009) 234–240.
[19] T. Ishida, K. Atobe, X. Wang, H. Kiwada, Accelerated blood clearance of PEGylated liposomes upon repeated injections: effect of doxorubicin-encapsulation and high-dose first injection, J. Control. Release. 115 (2006) 251–258.
[20] Y. Ge, H. Gao, X.T. Kong, Immunoglobulins and complement in splenectomised and autotransplanted subjects, Ann. Med. 21 (1989) 265–267.
[21] Y. Yasar, Y. Zeki, E. Ahmet, S. Metin, K. Huseyin, Plasma gamma globulin levels after splenectomy and spleen salvage, HPB. Surg. 1 (1989) 97–100.
[22] C.A. Janeway, P. Travers, M. Walport, M.J. Sholomchik, Immunobiology6 Ed, Garland Science Publishing, New York, 2005.
[23] G. Romano, Current development of nonviral-mediated gene transfer, Drug. News. Perspect. 20 (2007) 227–231.
[24] K. White, S.A. Nicklin, A.H. Baker, Novel vectors for in vivo gene delivery to vascular tissue, Expert. Opin. Biol. Ther. 7 (2007) 809–821.
[25] A.M. Krieg, CpG motifs in bacterial DNA and their immune effects, Annu. Rev. Immunol. 20 (2002) 709–760.
[26] S.L. Peng, Signaling in B cells via Toll-like receptors, Curr. Opin. Immunol. 17 (2005) 230–236.
[27] J.A. Harding, C.M. Engbers, M.S. Newman, N.I. Goldstein, S. Zalipsky, Immunogenicity and pharmacokinetic attributes of poly(ethylene glycol)-grafted immunoliposomes, Biochim. Biophys. Acta. 1327 (1997) 181–192.
[28] J.M. Harris, N.E. Martin, M. Modi, Pegylation: a novel process for modifying pharmacokinetics, Clin. Pharmacokinet. 40 (2001) 539–551.
[29] T. Ishida, H. Kiwada, Accelerated blood clearance (ABC) phenomenon upon repeated injection of PEGylated liposomes, Int. J. Pharm. 354 (2008) 56–62.
[30] S.C. Semple, T.O. Harasym, K.A. Clow, S.M. Ansell, S.K. Klimuk, M.J. Hope, Immunogenicity and rapid blood clearance of liposomes containing polyethylene glycol-lipid conjugates and nucleic Acid, J. Pharmacol. Exp. Ther. 312 (2005) 1020–1026.
[31] J.J. Mond, Q. Vos, A. Lees, C.M. Snapper, T cell independent antigens, Curr. Opin. Immunol. 7 (1995) 349–354.
[32] K.W. Moore, A. O'Garra, R. de Waal Malefyt, P. Vieira, T.R. Mosmann, Interleukin-10, Annu. Rev. Immunol. 11 (1993) 165–190.
[33] L.M. Pecanha, C.M. Snapper, A. Lees, H. Yamaguchi, J.J. Mond, IL-10 inhibits T cell-independent but not T cell-dependent responses in vitro, J. Immunol. 150 (1993) 3215–3223.
[34] K. Aschenbrenner, L.M. D'Cruz, E.H. Vollmann, M. Hinterberger, J. Emmerich, L.K. Swee, A. Rolink, L. Klein, Selection of Foxp3+ regulatory T cells specific for self antigen expressed and presented by Aire+ medullary thymic epithelial cells, Nat. Immunol. 8 (2007) 351–358.
[35] S.C. Hyde, I.A. Pringle, S. Abdullah, A.E. Lawton, L.A. Davies, A. Varathalingam, G. Nunez-Alonso, A.M. Green, R.P. Bazzani, S.G. Sumner-Jones, M. Chan, H. Li, N.S. Yew, S.H. Cheng, A.C. Boyd, J.C. Davies, U. Griesenbach, D.J. Porteous, D.N. Sheppard, F.M. Munkonge, E.W. Alton, D.R. Gill, CpG-free plasmids confer reduced inflammation and sustained pulmonary gene expression, Nat. Biotechnol. 26 (2008) 549–551.
[36] N.S. Yew, M. Przybylska, R.J. Ziegler, D. Liu, S.H. Cheng, High and sustained transgene expression in vivo from plasmid vectors containing a hybrid ubiquitin promoter, Mol. Ther. 4 (2001) 75–82.
[37] H. Zhao, H. Hemmi, S. Akira, S.H. Cheng, R.K. Scheule, N.S. Yew, Contribution of toll-like receptor 9 signaling to the acute inflammatory response to nonviral vectors, Mol. Ther. 9 (2004) 241–248.
[38] S. Li, S.P. Wu, M. Whitmore, E.J. Loeffert, L. Wang, S.C. Watkins, B.R. Pitt, L. Huang, Effect of immune response on gene transfer to the lung via systemic administration of cationic lipidic vectors, Am. J. Physiol. 276 (1999) L796–804.
[39] A.K. Yi, J.H. Chace, J.S. Cowdery, A.M. Krieg, IFN-gamma promotes IL-6 and IgM secretion in response to CpG motifs in bacterial DNA and oligonucleotides, J. Immunol. 156 (1996) 558–564.

Journal of Controlled Release 142 (2010) 167–173

Contents lists available at ScienceDirect

Journal of Controlled Release

journal homepage: www.elsevier.com/locate/jconrel

Sequential administration with oxaliplatin-containing PEG-coated cationic liposomes promotes a significant delivery of subsequent dose into murine solid tumor

Amr S. Abu Lila, Yusuke Doi, Kazuya Nakamura, Tatsuhiro Ishida *, Hiroshi Kiwada

Department of Pharmacokinetics and Biopharmaceutics, Subdivision of Biopharmaceutical Sciences, Institute of Health Biosciences, The University of Tokushima, 1-78-1, Sho-machi, Tokushima 770-8505, Japan

ARTICLE INFO

Article history:
Received 26 August 2009
Accepted 19 October 2009
Available online 25 October 2009

Keywords:
Anticancer therapy
Sequential administration
Anticancer drug
Oxaliplatin
PEG-coated cationic liposomes

ABSTRACT

Recently, we designed a PEG-coated cationic liposome to achieve dual targeting delivery of l-OHP to both tumor endothelial cells and tumor cells in a solid tumor. The targeted liposomal l-OHP formulation showed an efficient antitumor activity in a murine tumor model after three sequential liposomal l-OHP injections. This led us to assume that prior dosing with liposomes might enhance the intra-tumoral accumulation of a subsequent dose, and hence improve the therapeutic efficacy of entrapped l-OHP. The present study shows that while a single liposomal l-OHP injection does not enhance tumor accumulation of subsequent test-PEG-coated cationic liposomes, two sequential injections of liposomal l-OHP do. Cumulative cytotoxic effects of l-OHP delivered by PEG-coated cationic liposomes led to deep diffusion of a subsequent dose of liposomal l-OHP in solid tumor presumably as a result of the enlarged intra-tumoral interstitial space. Our study suggests that sequential injections of a targeted liposomal anticancer drug is of significant clinical and practical importance in enhancing the delivery of adequate quantities of anticancer agents into intractable solid tumors, and thereby may achieve a significant anticancer efficacy.

1. Introduction

The use of most chemotherapeutic agents is mainly restrained by either their indiscriminate toxicity towards healthy tissues or their limited ability to penetrate tumor tissue in a significantly effective concentration [1–3]. Therefore, it would be highly desirable to develop drug delivery systems that selectively target drugs to tumor tissue [4–7].

A variety of drug delivery systems have been developed. Of these, the liposomal drug delivery system represents an advanced and versatile system for selective delivery of anti-cancer drugs to solid tumors by altering the pharmacokinetics and biodistribution pattern of the encapsulated drug [8–10]. Many liposome-based drug delivery systems encapsulating chemotherapeutic agents have exerted an efficient antitumor activity in the pre-clinical studies after successive injections of the liposomal formulation, but not after a single injection [11–13].

It is believed that such efficient antitumor activity can be attributed to the selective delivery and the preferential accumulation of liposomal anticancer drug in tumor tissue via the enhanced permeability and retention (EPR) effect [14–16]. However, an important yet-little appreciated factor that might be involved in the antitumor efficiency of liposomal anticancer drug is the enhancing effect of the primary dose on the accumulation of subsequently injected doses. Anticancer drug, released from the primary dose of liposomes staying in the tumor tissue, may alter the tumor microenvironment as a result of killing viable tumor cells and tumor endothelial cells. Consequently, this will allow the deep penetration of the subsequently injected liposomal anticancer drug, which will result in a further increased antitumor efficacy. However, thus far only very few reports have demonstrated the effect of prior dosing of a liposomal anticancer drug on the accumulation of subsequently doses.

We recently developed a polyethylene glycol (PEG)-coated cationic liposome [17] and confirmed that l-OHP encapsulated in such liposomes was effective in suppressing tumor growth via a dual targeting mechanism against both tumor endothelial cells and tumor cells in tumor-bearing mice [18]. This effect was achieved after three sequential injections of liposomal l-OHP [18]. On the basis of this observation, we assumed that first or/and second injection of liposomal l-OHP might enhance the intra-tumor accumulation of subsequent doses by allowing secondary doses of liposomes to penetrate deeply into the solid tumor, hence improving the overall therapeutic efficiency of l-OHP.

In the present study we followed the biodistribution and intra-tumor accumulation of PEG-coated cationic liposomes after either a single or two subsequent injection(s) of l-OHP-containing PEG-coated cationic liposomes. The results indicated that sequential administration of liposomal chemotherapeutic agents has a significant promoting effect

Abbreviations: CHOL, cholesterol; DC-6-14, O,O′-ditetradecanoyl-N-(alpha trimethyl ammonioacetyl)diethanolamine chloride; DiI, 1,1′-dioctadecyl-3,3,3′,3′-tetramethylin-docarbocyanine perchlorate; DMEM, Dulbecco's modified Eagle's medium; FBS, fetal bovine serum; HSPC, hydrogenated soya phosphatidylcholine; LLCC, Lewis lung carcinoma cells; l-OHP, oxaliplatin; $mPEG_{2000}$-DSPE, 1,2-distearoyl-sn-glycero-3-phosphoethanolamine-*n*-[methoxy (polyethyl-eneglycol)-2000]; PBS, phosphate buffered saline; ^{3}H-CHE, tritium-cholesterylhexadecyl ether.

* Corresponding author. Tel./fax: +81 88 633 7260.
E-mail address: ishida@ph.tokushima-u.ac.jp (T. Ishida).

0168-3659/$ – see front matter © 2009 Elsevier B.V. All rights reserved.
doi:10.1016/j.jconrel.2009.10.020

on the accumulation of the subsequently administered dose within a solid tumor, thereby promoting an enhanced anticancer effect of the encapsulated anticancer agents.

2. Materials and methods

2.1. Materials

Hydrogenated soy phosphatidylcholine (HSPC) and 1,2-distearoyl-sn-glycero-3-phosphoethanolamine-*n*-[methoxy (polyethyleneglycol)-2000] ($mPEG_{2000}$-DSPE) were generously donated by NOF (Tokyo, Japan). Oxaliplatin (l-OHP) was generously donated by Taiho Pharmaceutical (Tokyo, Japan). Cholesterol (CHOL) was purchased from Wako Pure Chemical (Osaka, Japan). O,O′-ditetradecanoyl-N-(alpha-trimethyl ammonio acetyl) diethanolamine chloride (DC-6-14) was purchased from Sogo Pharmaceutical (Tokyo, Japan). 1,1′-dioctadecyl-3,3,3′,3′-tetramethylindocarbocyanine perchlorate (DiI) was purchased from Invitrogen (OR, USA). ^{3}H-Cholesterylhexadecyl ether (^{3}H-CHE) was purchased from PerkinElmer Life Science (MA, USA). All other reagents were of analytical grade.

2.2. Animals and tumor cell line

Male C57BL/6 mice, 4 weeks old, were purchased from Japan SLC (Shizuoka, Japan). The experimental animals were allowed free access to water and mouse chow, and were housed under controlled environmental conditions (constant temperature, humidity, and 12 h dark-light cycle). All animal experiments were evaluated and approved by the Animal and Ethics Review Committee of the University of Tokushima. Lewis lung carcinoma cell (LLCC) line was purchased from Cell Resource Center for Biomedical Research (Institute of Development, Aging and Cancer, Tohoku University) and maintained in Dulbecco's modified Eagle's medium (DMEM) (Nissui Pharmaceutical, Tokyo, Japan) supplemented with 10% heat-inactivated FBS (Japan Bioserum, Hiroshima, Japan), 10 mM L-glutamine, 100 U/ml penicillin and 100 μg/ml streptomycin in a 5% CO_2 air incubator at 37 °C.

2.3. Preparation of liposomes

Cationic liposomes modified with $mPEG_{2000}$-DSPE were composed of HSPC/CHOL/DC-6-14/$mPEG_{2000}$-DSPE (2/1/0.2/0.2 molar ratio). Neutral liposomes modified with $mPEG_{2000}$-DSPE were composed of HSPC/CHOL/$mPEG_{2000}$-DSPE (2/1/0.2 molar ratio). To follow the biodistribution of the liposomes, the liposomes were labeled with a trace amount of ^{3}H-CHE (40 μCi/μmol lipid) as a non-exchangeable lipid phase marker. For in vivo imaging experiments, 1 mol% of the fluorescent dye DiI was incorporated in the lipid mixture. All liposomes were prepared according to the method described earlier [17]. Briefly, lipids (50 mmol) were dissolved in 6 ml of chloroform/diethyl ether (1:2 v/v) and then 2 ml of l-OHP solution (8 mg/ml) in 5% (w/v) dextrose was added dropwise into the lipid mixture to form a w/o emulsion. For preparation of empty PEG-coated liposomes, 5% dextrose solution was added instead of l-OHP solution. The volume ratio of the aqueous to the organic phase was maintained at 1:3. The emulsion was sonicated for 15 min and then the organic phase was removed to form liposomes by evaporation in a rotary evaporator at 40 °C under reduced pressure at 250 hPa for 1 h. The resulting liposomes were extruded through a polycarbonate membrane (200 nm pore size) using an extruder device (Lipex Biomembranes Inc., Vancouver, Canada) maintained at 65 °C to obtain liposomes with approximately 200 nm in a mean diameter. The phospholipid concentration was determined by colorimetric assay [19]. Unencapsulated, free l-OHP was removed by dialysis by means of a dialysis cassette (Slyde-A-Lyzer, 10000MWCO, PIERCE, IL, USA) against 5% dextrose. Encapsulated l-OHP was quantified using an atomic absorption photometer (Z-5700, Hitachi, Tokyo, Japan). The size and zeta potential of the liposomes were determined at 25 °C and pH 7.4 by using a NICOMP 370 HPL submicron particle analyzer (Particle Sizing System, CA, USA). The encapsulation efficiency of l-OHP was calculated by dividing the drug to lipid ratio after the dialysis by the initial drug to lipid ratio.

2.4. Biodistribution study in tumor-bearing mice

To assess the tissue distribution of either PEG-coated cationic liposomes or PEG-coated neutral liposomes, male C57BL/6 mice were inoculated subcutaneously (s.c.) at the flank region with 5×10^5 LLCC in 100 μl PBS. On day 12 after tumor inoculation, mice were intravenously injected via the tail vein with either ^{3}H-CHE-labeled PEG-coated cationic liposomes or ^{3}H-CHE-labeled PEG-coated neutral liposomes at a dose of 125 mg total lipid/kg body weight. At selected post-injection time points (5 min, 30 min, 1 h, 2 h, 4 h, 6 h, 24 h, and 48 h), blood (100 μl) was collected from the retro-orbital sinus. After withdrawing blood samples, mice were sacrificed and then liver, spleen, lung, kidney and tumor were collected. Tissue samples were washed with cold phosphate buffered saline (PBS, 37 mM NaCl, 2.7 mM KCl, 8.1 mM Na_2HPO_4 and 1.47 mM KH_2PO_4; pH 7.4) and weighed after removing excess fluid. Radioactivity in blood and tissues was assayed as described previously [20]. Pharmacokinetic parameters were calculated using poly-exponential curve fitting and the least-squares parameter estimation program SAAM II (Micromath, UT, USA).

2.5. In vivo fluorescence imaging study

LLCC were inoculated subcutaneously as described above. On day 12 after tumor inoculation, mice received either DiI-labeled PEG-coated cationic liposomes or DiI-labeled PEG-coated neutral liposomes (125 mg lipid/kg) via the tail vein. At 6, 24 and 48 h post-injection, mice were anesthetized with isoflurane (FORANE, Abott Japan, Osaka, Japan), a short acting anesthetic, and maintained throughout the imaging process on a heating pad at 37 °C. Fluorescence imaging was performed with Fluorescence Image Analyzer LAS-4000IR (Fujifilm, Tokyo, Japan). The fluorescence images were acquired with a 1/8 s exposure time.

2.6. Effect of liposomal l-OHP injections on tumor accumulation of test-PEG-coated liposomes

To evaluate the effect of liposomal l-OHP injections on the accumulation of subsequently injected liposomes, test liposomes were injected into tumor-bearing mice following either a single or two liposomal l-OHP injections. Tumor-bearing mice were divided into four groups with 4 animals in each group.

Group I. Single injection of l-OHP containing PEG-coated cationic liposomes (5 mg l-OHP/kg) on day 8 after tumor inoculation. Four days later, either ^{3}H-CHE-labeled or DiI-labeled PEG-coated cationic liposomes were intravenously injected (125 mg lipid/kg).

Group II. Single injection of l-OHP containing PEG-coated neutral liposomes (5 mg l-OHP/kg) on day 8 after tumor inoculation. Four days later, either ^{3}H-CHE-labeled or DiI-labeled PEG-coated neutral liposomes were intravenously injected (125 mg lipid/kg).

Group III. Two sequential injections of l-OHP containing PEG-coated cationic liposomes (5 mg l-OHP/kg) on days 8 and 12 after tumor inoculation. Four days later, either ^{3}H-CHE-labeled or DiI-labeled PEG-coated cationic liposomes were intravenously injected (125 mg total lipid/kg).

Group IV. Two sequential injections of l-OHP containing PEG-coated neutral liposomes (5 mg l-OHP/kg) on days 8 and 12 after

tumor inoculation. Four days later, either ^{3}H-CHE-labeled or DiI-labeled PEG-coated neutral liposomes were intravenously injected (125 mg total lipid/kg).

For a quantitative study of liposome distribution, mice were sacrificed at 6, 24 and 48 h after injection of ^{3}H-CHE-labeled PEG-coated liposomes. Tumors were excised and radioactivity in tumor tissues was assayed as described previously [19]. For a qualitative study of liposome distribution, both in vivo imaging of liposome distribution and histological examination of tumor section were performed. To study in vivo imaging of liposome distribution, mice were anesthetized at defined time periods (6, 24 and 48 h) after injection of DiI-labeled liposomes injection. Fluorescence imaging was performed as described above with Fluorescence Image Analyzer LAS-4000IR (Fujifilm, Tokyo, Japan). The fluorescence images were acquired with a 1/8 s exposure time. To perform histological examination of tumor sections, mice were sacrificed 24 h post test-DiI-labeled liposome injection. The tumors were excised and snap-frozen in OCT compound (Sakura Fintechnical, Tokyo, Japan) by dry-iced acetone. Frozen samples were cut into sections of 10-μm thickness in a cryostat (Leica Microsystems, Solms, Germany), mounted on a glass slide and dried in air. The samples were then examined under fluorescence microscopy (Axioimager A1, Zeiss, Oberkohen, Germany).

2.7. Statistical analysis

All values are expressed as mean ± S.D. Statistical analysis was performed with a two-tailed unpaired t test and one way ANOVA using Graphpad InStat software (GraphPad Software, CA, USA). The level of significance was set at $p<0.05$.

3. Results

3.1. Characterization of liposomes

The average size of PEG-coated cationic liposomes was 201 ± 11.3 nm and the zeta potential was +11.3 ± 0.8 mV. The size of PEG-coated neutral liposomes (control liposomes) was 202 ± 13.2 nm and the zeta potential was −6.3 ± 1.1 mV. The encapsulation efficiency of l-OHP was 22.3 ± 2.2% for PEG-coated cationic liposomes and 18.1 ± 2.9% for PEG-coated neutral liposomes.

3.2. Blood clearance and organ distribution of PEG-coated liposomes

The pharmacokinetic profile and organ distribution of both PEG-coated cationic liposomes and PEG-coated neutral liposomes were evaluated in mice bearing a LLCC tumor xenograft. Both liposomes showed prolonged blood circulation with half-lives of 10.4 ± 0.7 and 9.4 ± 0.5 h, respectively (Fig. 1A and Table 1). The percent dose of the lipid remaining in the blood at 24 h was similar for PEG-coated cationic liposomes (12.7 ± 1.7 (%)) and PEG-coated neutral liposomes (11.2 ± 1.8 (%)) (Fig. 1A). However, PEG-coated cationic liposomes showed a lower area under the blood concentration versus time curve (AUC) than PEG-coated neutral liposomes ($p<0.01$) (Fig. 1A and Table 1). Apparently, the presence of surface positive charge enhances both blood clearance (Clearance) and tissue distribution (V_d) of PEG-coated cationic liposomes (Table 1).

As shown in Fig. 1B, PEG-coated cationic liposomes and PEG-coated neutral liposomes accumulated in liver and spleen to similar extents. This demonstrates that PEGylation of the cationic liposomes effectively prevents the rapid clearance of cationic liposomes from the blood circulation as is observed for non-PEGylated cationic liposomes.

Tumor accumulation of test liposomes was determined as a function of time following intravenous injection (Fig. 2). In tumor-bearing mice not treated with l-OHP liposome (control), PEG-coated cationic liposomes showed 2–3 fold higher accumulation in tumor

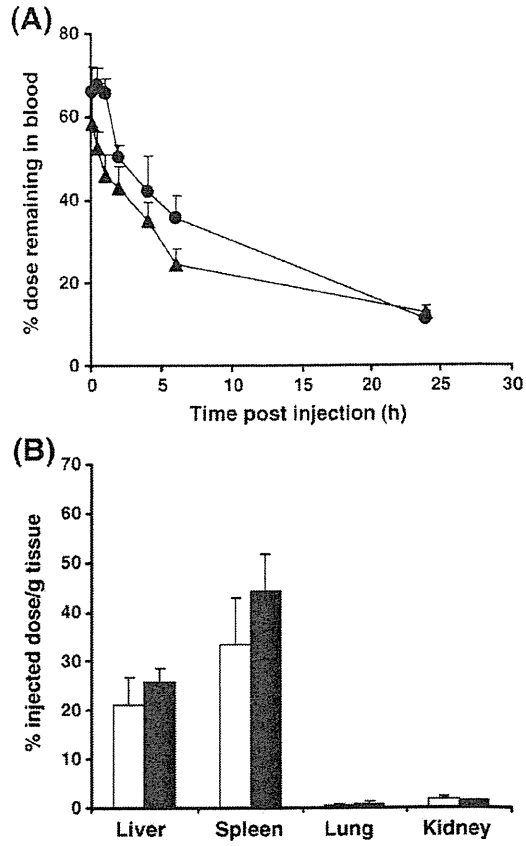

Fig. 1. Blood clearance and organ distribution of PEG-coated liposomes. On day 12 after tumor inoculation, LLCC tumor-bearing mice ($n=4$) were injected intravenously with either radio-labeled PEG-coated cationic or neutral liposomes. At selected time points (0.083, 0.5, 1, 2, 4, 6, and 24 h), blood was collected and analyzed for radioactivity. At 24 h post-injection, the radioactivity in each organ was determined. Data are presented as mean ± SD. (In the case of spleen, the value was per 500 mg instead of per gram). (A) represents blood clearance of PEG-coated cationic liposomes (▲) versus PEG-coated neutral liposomes (●). (B) represents organ distribution of PEG-coated cationic liposomes (closed columns) and PEG-coated neutral liposomes (open columns).

tissue than PEG-coated neutral liposomes ($p<0.001$). Interestingly, tumor accumulation of PEG-coated cationic liposomes tended to increase up to 24 h after injection, and remained at this level even at 48 h after injection. Tumor accumulation of PEG-coated neutral liposomes, on the other hand, was substantially lower and reached a maximum at 24 h post-injection followed by a gradual decline during the next 24 h ($p<0.01$).

Fig. 3 represents blood and organ distribution of test-PEG-coated cationic liposomes and test-PEG-coated neutral liposomes after either single (Fig. 3A) or two (Fig. 3B) pretreatments with liposomal l-OHP. It is clear that there were no significant differences in blood and organ

Table 1
Pharmacokinetic parameters of PEG-coated liposomes in tumor-bearing mice.

Liposome	Half-life (h)	Clearance (ml/h)	$AUC_{t=0\to\infty}$ (%dose·h/ml)	V_d (ml)
PEG-coated cationic liposomes	10.4 ± 0.7^{ns}	0.133 ± 0.007*	750.6 ± 35.2*	1.99 ± 0.10**
PEG-coated neutral liposomes	9.4 ± 0.5	0.113 ± 0.005	884.9 ± 41.7	1.53 ± 0.07

LLCC tumor-bearing mice received a single intravenous injection of either radio-labeled PEG-coated cationic liposomes or radio-labeled PEG-coated neutral liposomes. Pharmacokinetic variables were determined using PK Analyst software. Data represent the mean ± SD ($n=4$ mice per time point). ns > 0.05, *$p<0.05$, **$p<0.01$ against PEG-coated neutral liposomes.

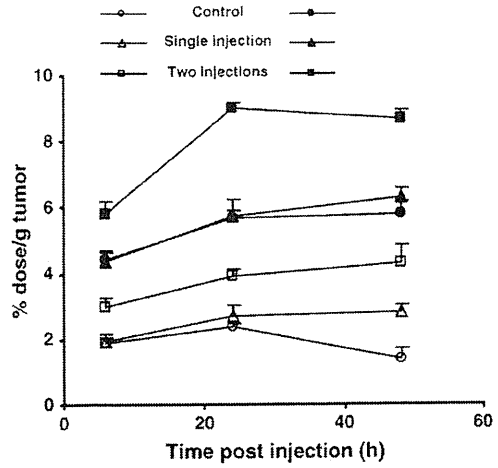

Fig. 2. Intra-tumoral accumulation of PEG-coated test liposomes after sequential liposomal l-OHP administration. LLCC tumor-bearing mice received either a single or two sequential injection(s) of liposomal l-OHP every 4 days. Four days later, the treated mice received either radio-labeled PEG-coated cationic (closed symbols) or neutral (open symbols) liposomes. Mice receiving only the radio-labeled PEG-coated liposomes served as controls. At 6, 24, and 48 h post-injection, the radioactivity in tumors was determined. Data are presented as the percentage of the injected dose per gram of tumor tissue and SD ($n=4$).

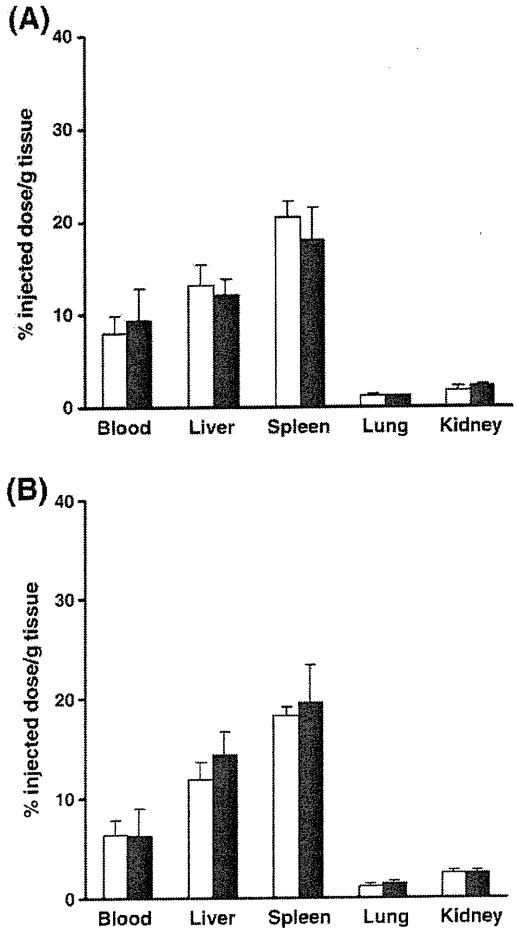

Fig. 3. Blood and organ distribution of PEG-coated test liposomes after sequential liposomal l-OHP administration. LLCC tumor-bearing mice received either a single (A) or two (B) sequential injection(s) of liposomal l-OHP with 4 days interval. Four days later, the treated mice received either test-PEG-coated cationic (closed columns) or neutral (open columns) liposomes. At 24 h post-injection, the radioactivity in blood and each organ was determined. Data are presented as mean ± SD. (In the case of blood, the value was per ml, and in the case of spleen, the value was per 500 mg instead of per gram).

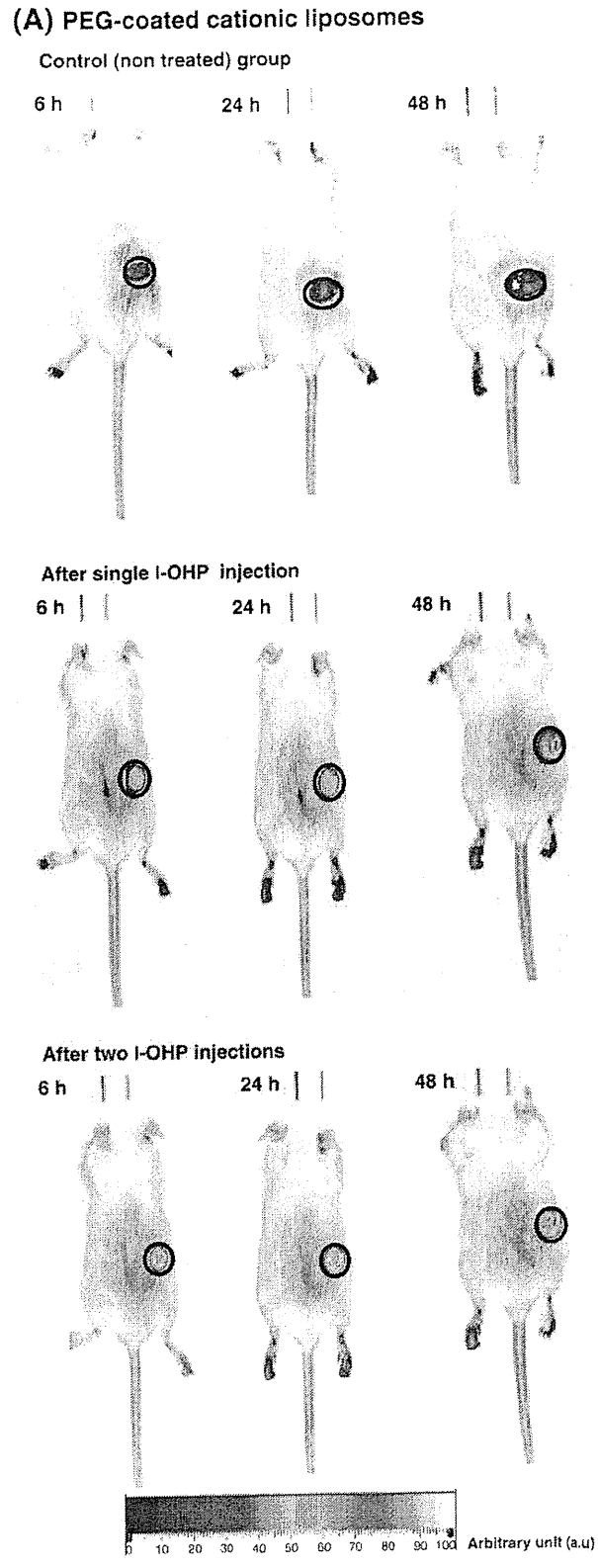

Fig. 4. In vivo tumor distribution of fluorescently labeled PEG-coated liposomes. LLCC tumor-bearing mice were pretreated with either a single or two sequential injection(s) of liposomal l-OHP every 4 days. Four days later, the treated mice received an intravenous injection of fluorescent (DiI) labeled-PEG-coated liposomes. Mice receiving only the DiI-labeled PEG-coated liposomes served as controls. At 6, 24, and 48 h post injection, in vivo optical images were recorded. (A) DiI-labeled PEG-coated cationic liposomes. (B) DiI-labeled PEG-coated neutral liposomes. All fluorescence images were acquired with a 1/8 s exposure time. Circles indicate tumor locations, not exact tumor areas.

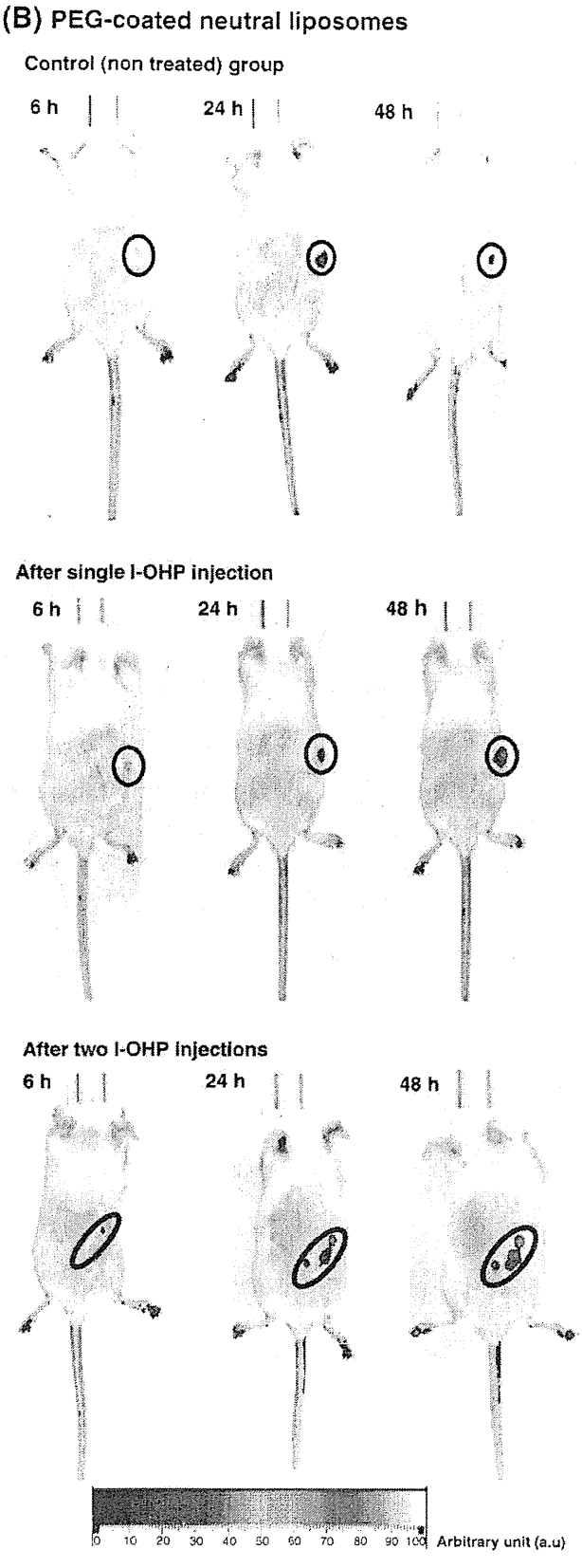

Fig. 4 (*continued*).

distribution of both cationic and neutral liposomes upon pretreatment with either a single or two injections of liposomal l-OHP.

3.3. *Effect of prior-injection(s) of liposomal l-OHP on tumor accumulation of subsequently injected test-PEG-coated liposomes*

The effect of a single liposomal l-OHP injection on the tumor accumulation of subsequently injected test liposomes is also presented in Fig. 2. In mice pretreated with a single liposomal l-OHP injection, the tumor accumulation levels of both test-PEG-coated cationic liposomes and test-PEG-coated neutral liposomes were similar to those in non-treated (control) mice ($p > 0.05$) except for the accumulation of neutral liposomes at 48 h post-injection, which remained at the 24-h level instead of decreasing.

In mice pretreated with two successive injections of liposomal l-OHP, the tumor accumulation of both cationic and neutral test liposomes was significantly higher than that in non-treated (control) mice ($p < 0.001$) or in mice pretreated with a single injection ($p < 0.01$). In addition, as a function of time post test-dose injection, the tumor accumulation of both cationic and neutral test liposomes was in the following order of time post-injection: 48 h ≥ 24 h ≫ 6 h.

3.4. *In vivo imaging study on intra-tumoral accumulation of PEG-coated liposomes*

The effect of sequential injections of liposomal l-OHP on the intra-tumoral distribution of cationic and neutral liposomes was visualized using an in vivo imaging system. Representative images are presented in Fig. 4. Through the experiment, mice that had received cationic test liposomes (Fig. 4A)showed a larger and broader intra-tumoral distribution of fluorescence, representative of the distribution of liposomes, than mice that had received neutral test liposomes (Fig. 4B). Pretreatment with two successive injections of l-OHP-

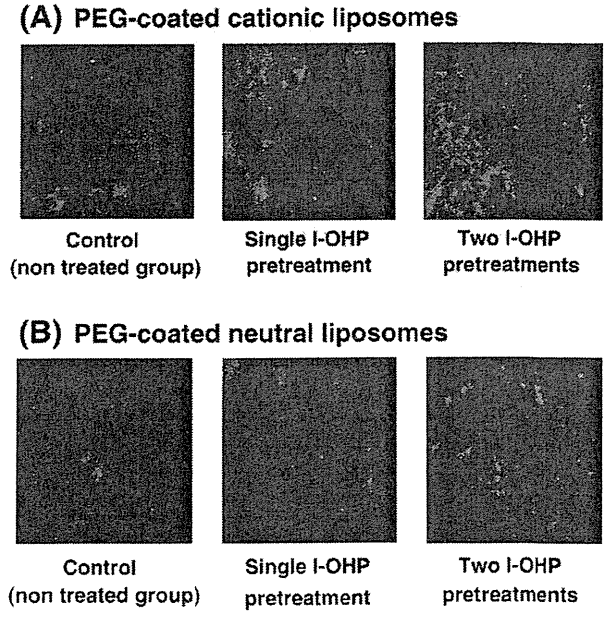

Fig. 5. Histological examination on intra-tumor distribution of fluorescently labeled PEG-coated liposomes. LLCC tumor-bearing mice were pretreated with either a single or two sequential injection(s) of liposomal l-OHP with 4 days interval. Four days later, the treated mice received an intravenous injection of DiI-labeled PEG-coated liposomes. Mice receiving only the DiIlabeled PEG-coated liposomes served as controls. At 24 h post-injection, mice were sacrificed. Tumor was excised and snap frozen. Frozen samples were cut into sections of 10-μm thickness and were then examined under fluorescence microscopy. (A) DiI-labeled PEG-coated cationic liposome. (B) DiI-labeled PEG-coated neutral liposome. Red spots represent liposomal distribution. Magnification, ×100.

containing PEG-coated cationic liposomes resulted in a broader and homogenous intra-tumoral distribution of the subsequently injected test dose. Pretreatment with a single injection of l-OHP-containing PEG-coated cationic liposomes slightly enhanced the distribution of cationic test liposomes in the tumor. On the other hand, mice pretreated either once or twice with l-OHP-containing PEG-coated neutral liposomes showed only a limited and heterogeneous (separate patches) intra-tumoral distribution of test dose liposomes.

3.5. Histological examination of tumor sections upon pretreatment with liposomal l-OHP

Liposomal distribution in the tumor was determined from fluorescence microscopy images of four to five tumors (Fig. 5). Sequential administration of either PEG-coated cationic liposomes or PEG-coated neutral liposomes was found to enhance broader distribution of subsequently injected dose given that mice pretreated with two liposomal l-OHP injections showing higher distribution than mice pretreated with only a single liposomal l-OHP injection. Moreover, mice pretreated with PEG-coated cationic liposomes showed a higher distribution levels than mice treated with PEG-coated neutral liposomes.

4. Discussion

To obtain sufficient antitumor activity with liposomal anticancer drugs, optimization of the therapeutic regimen is of great importance. However, there are only a few reports in literature dealing with the design of regimens for the administration of liposomal anticancer drugs. We recently designed a PEG-coated cationic liposome containing 1-OHP and demonstrated that such liposomal l-OHP formulation has a potent in vivo antitumor activity, presumably via a dual targeting approach against both tumor endothelial cells and tumor cells [17]. Interestingly, such efficient antitumor activity was achieved only after three sequential intravenous injections [18]. Therefore, a key objective of this study was to investigate the effect of sequential administration of l-OHP-containing PEG-coated cationic liposomes on the delivery of l-OHP to tumor tissue, and its implication with respect to overall antitumor activity.

Biodistribution studies (Fig. 2), in vivo imaging studies (Fig. 4) and histopathological study (Fig. 5) demonstrated that two successive injections of liposomal l-OHP allowed enhanced accumulation and broader distribution of subsequently injected PEG-coated cationic test liposomes in tumor tissue. This might be attributed to the cumulative cytotoxic effect of the pre-injected liposomal l-OHP formulation on both endothelial cells and tumor cells. l-OHP-containing PEG-coated cationic liposomes, because of their prolonged circulation time in the blood, are likely to have easy access to tumor endothelial cells and to readily extravasate subsequently from the blood stream into the tumor interstitial space thus gaining access to the tumor cells. Once in the tumor tissue, l-OHP-containing liposomes can be internalized by both tumor endothelial cells and tumor cells following interaction with those cells, as demonstrated earlier [18]. Thus, liposomal l-OHP will be allowed to exert its cytotoxic effect [21,22] and may bring about a decrease in the number of tumor cells and, consequently, a decrease in tumor interstitial pressure, thus allowing deeper penetration of the cationic test liposomes (Figs. 2, 4 and 5).

Remarkably, a single injection of l-OHP-containing PEG-coated cationic liposomes did not enhance the intra-tumoral accumulation of the subsequently injected test dose (Fig. 2). This might be due to the insufficient delivery of l-OHP to tumor tissue or/and a sub-optimal time interval between doses. After a single injection the fraction of the dose of l-OHP-containing PEG-coated cationic liposomes that reached the tumor tissue, seemed to become almost entirely bound to tumor endothelial cells while only a small proportion remained available for extravasation into the tumor interstitium. This relatively small fraction of liposomal l-OHP extravasating in the interstitial space of tumor tissue might be insufficient to exert a potent cytotoxic effect against the tumor cells and thus failed to enhance the intra-tumoral accumulation of the subsequently injected second dose. In addition, the time interval (four days) between the doses might be insufficient for l-OHP to be released from the liposomes in a sufficiently high concentration to exert a cytotoxic effect against viable tumor cells.

PEG-coated neutral liposomes (Stealth liposomes) have been widely used to achieve a passive targeting of anticancer drugs to tumor tissue [23–25]. Doxorubicin-containing PEG-coated neutral liposomes, Doxil/Caelyx, have been approved for clinical use [26,27]. In this study, PEG-coated neutral liposomes showed lower intra-tumoral accumulation (Fig. 2) than PEG-coated cationic liposomes. This is most likely related to the lower association of such liposomes with tumor endothelial cells and the rapid elimination from tumor tissues due to the lack of anchor (electric force) to endothelial cells and/or tumor cells, when compared with PEG-coated cationic liposomes. Interestingly, upon pretreatment with either single or two liposomal l-OHP injections, the accumulation level of PEG-coated neutral liposomes at 48-h post-injection remained at the 24-h level instead of decreasing. This might be attributed to the impairment of liposomal clearance via lymphatic drainage due to suppressing tumor lymphogenesis by pretreatment with liposomal l-OHP. Recently several attempts have been reported to extend retention time of PEG-coated neutral liposomes in tumor tissue. These attempts relied on active targeting of such liposomes to tumor tissue via conjugation of tumor-targeting ligands at the surface of liposomes [28–30]. These tumor-targeting ligands include small-molecular ligands (such as folate and some vitamins [31,32]), peptides (such as Arg-Gly-Asp [33] and sequences identified by phage display [34]), proteins (such as hormones), transferrin [35,36], antibodies and antibody fragments [37], and oligosaccharides [38].

It appeared from our study that intra-tumoral accumulation of l-OHP-containing PEG-coated cationic liposomes is dependent on the dosing schedule. Administering liposomal l-OHP every four days significantly enhanced the intra-tumoral accumulation of subsequently injected dose (Figs. 2 and 4), and thereby increased the therapeutic efficacy [18], without causing marked toxicity. In contrast, administering liposomal l-OHP every two or three days caused severe systemic toxicity resulting in death of almost all mice within 20–25 days (not shown). Although there has not been yet any evidence to support the concern, we assume that sequential administration of l-OHP-containing PEG-coated cationic liposomes at short-intervals leads to saturation of binding sites and/or accumulation space of the liposomes in the tumor tissue. Consequently, additionally administered liposomal l-OHP accumulates in normal tissues, leading to severe systemic toxicity of l-OHP.

For efficient intra-tumoral accumulation, liposomes should be able to leave the blood compartment efficiently and then penetrate deeply into the tumor tissue so as to reach all the cancer cells [39,40]. However, liposomal diffusion into tumor tissues may face a number of barriers which may frustrate its efficient penetration throughout the tumor tissue. Au et al. [41,42] reported that alteration of tumor microenvironment by decreasing tumor cell density with subsequent reduction in tumor interstitial pressure enhances intra-tumoral accumulation of injected free, i.e. not carrier-associated anticancer drugs. Here, we propose that sequential treatments with targeted liposomes containing an anticancer drug using an optimal dosing schedule further enhance therapeutic efficiency as a result of enhanced tumor penetration of subsequent doses by decreasing tumor cell density and allowing deep diffusion throughout tumor tissue.

5. Conclusion

In this study, we confirmed that sequential injections of l-OHP-containing PEG-coated cationic liposomes enhance intra-tumor accumulation of subsequently injected liposome doses (especially the third dose).

We tentatively ascribed this to the cumulative cytotoxic effect of the pre-injected liposomal l-OHP formulations on both endothelial cells and tumor cells, leading to deep penetration of the test-PEG-coated cationic liposomes as a result of a decrease in the density of tumor cells followed by a decrease in tumor interstitial pressure. Our results may indicate that sequential injection of a targeted liposomal anticancer drug is of significant clinical and practical relevance as it enhances the delivery of adequate quantities of anticancer agents into intractable solid tumors, provided that the dosage regimens are optimized.

Acknowledgments

We thank Dr. G.L. Scherphof for his helpful advice in preparing this manuscript. This study was supported, in part, by Grant-in-Aid for Young Scientists (A) (21689002), the Ministry of Education, Culture, Sports, Science and Technology, Japan.

References

[1] F. Yuan, M. Leunig, S.K. Huang, D.A. Berk, D. Papahadjopoulos, R.K. Jain, Microvascular permeability and interstitial penetration of sterically stabilized (stealth) liposomes in a human tumor xenograft, Cancer Res. 54 (1994) 3352–3356.
[2] R.K. Jain, Delivery of molecular and cellular medicine to solid tumors, Adv. Drug Deliv. Rev. 26 (1997) 71–90.
[3] R.K. Jain, Delivery of molecular and cellular medicine to solid tumors, J. Control. Release 53 (1998) 4967.
[4] M. Karita, H. Tsuchiya, M. Kawahara, S. Kasaoka, K. Tomita, The antitumor effect of liposome-encapsulated cisplatin on rat osteosarcoma and its enhancement by caffeine, Anticancer Res. 28 (2008) 1449–1457.
[5] T. Lammers, W.E. Hennink, G. Storm, Tumour-targeted nanomedicines: principles and practice, Br. J. Cancer 99 (2008) 392–397.
[6] M. Hong, S. Zhu, Y. Jiang, G. Tang, Y. Pei, Efficient tumor targeting of hydroxycamptothecin loaded PEGylated niosomes modified with transferrin, J. Control. Release 133 (2009) 96–102.
[7] H. Zhao, J.C. Wang, Q.S. Sun, C.L. Luo, Q. Zhang, RGD-based strategies for improving antitumor activity of paclitaxel-loaded liposomes in nude mice xenografted with human ovarian cancer, J. Drug Target. 17 (2009) 10–18.
[8] X.B. Xiong, Y. Huang, W.L. Lu, X. Zhang, H. Zhang, T. Nagai, Q. Zhang, Intracellular delivery of doxorubicin with RGD-modified sterically stabilized liposomes for an improved antitumor efficacy: in vitro and in vivo, J. Pharm. Sci. 94 (2005) 1782–1793.
[9] S. Hussain, A. Pluckthun, T.M. Allen, U. Zangemeister-Wittke, Antitumor activity of an epithelial cell adhesion molecule targeted nanovesicular drug delivery system, Mol. Cancer Ther. 6 (2007) 3019–3027.
[10] W. Sun, W. Zou, G. Huang, A. Li, N. Zhang, Pharmacokinetics and targeting property of TFu-loaded liposomes with different sizes after intravenous and oral administration, J. Drug Target. 16 (2008) 357–365.
[11] C.M. Lee, T. Tanaka, T. Murai, M. Kondo, J. Kimura, W. Su, T. Kitagawa, T. Ito, H. Matsuda, M. Miyasaka, Novel chondroitin sulfate-binding cationic liposomes loaded with cisplatin efficiently suppress the local growth and liver metastasis of tumor cells in vivo, Cancer Res. 62 (2002) 4282–4288.
[12] K. Morimoto, M. Kondo, K. Kawahara, H. Ushijima, Y. Tomino, M. Miyajima, J. Kimura, Advances in targeting drug delivery to glomerular mesangial cells by long circulating cationic liposomes for the treatment of glomerulonephritis, Pharm. Res. 24 (2007) 946–954.
[13] T. Asai, S. Miyazawa, N. Maeda, K. Hatanaka, Y. Katanasaka, K. Shimizu, S. Shuto, N. Oku, Antineovascular therapy with angiogenic vessel-targeted polyethyleneglycol-shielded liposomal DPP-CNDAC, Can. Sci. 99 (2008) 1029–1033.
[14] Y. Matsumura, H. Maeda, A new concept for macromolecular therapeutics in cancer chemotherapy: mechanism of tumoritropic accumulation of proteins and the antitumor agent smancs, Cancer Res. 46 (1986) 6387–6392.
[15] J.H. Kim, Y.S. Kim, S. Kim, J.H. Park, K. Kim, K. Choi, H. Chung, S.Y. Jeong, R.W. Park, I.S. Kim, I.C. Kwon, Hydrophobically modified glycol chitosan nanoparticles as carriers for paclitaxel, J. Control. Release 111 (2006) 228–234.
[16] H. Maeda, G.Y. Bharate, J. Daruwalla, Polymeric drugs for efficient tumor-targeted drug delivery based on EPR-effect, Eur. J. Pharm. Biopharm. 71 (2009) 409–419.
[17] A. Abu-Lila, T. Suzuki, Y. Doi, T. Ishida, H. Kiwada, Oxaliplatin targeting to angiogenic vessels by PEGylated cationic liposomes suppresses the angiogenesis in a dorsal air sac mouse model, J. Control. Release 134 (2009) 18–25.
[18] A.S. Abu Lila, S. Kizuki, Y. Doi, T. Suzuki, T. Ishida, H. Kiwada, Oxaliplatin encapsulated in PEG-coated cationic liposomes induces significant tumor growth suppression via a dual-targeting approach in a murine solid tumor model, J. Control. Release 137 (2009) 8–14.
[19] G.R. Bartlett, Colorimetric assay methods for free and phosphorylated glyceric acids, J. Biol. Chem. 234 (1959) 469–471.
[20] H. Harashima, C. Yamane, Y. Kume, H. Kiwada, Kinetic analysis of AUC-dependent saturable clearance of liposomes: mathematical description of AUC dependency, J. Pharmacokinet. Biopharm. 21 (1993) 299–308.
[21] S. Arnould, S. Guichard, I. Hennebelle, G. Cassar, R. Bugat, P. Canal, Contribution of apoptosis in the cytotoxicity of the oxaliplatin-irinotecan combination in the HT29 human colon adenocarcinoma cell line, Biochem. Pharmacol. 64 (2002) 1215–1226.
[22] M. Eriguchi, Y. Nonaka, H. Yanagie, I. Yoshizaki, Y. Takeda, M. Sekiguchi, A molecular biological study of anti-tumor mechanisms of an anti-cancer agent oxaliplatin against established human gastric cancer cell lines, Biomed. Pharmacother. 57 (2003) 412–415.
[23] P.J. Photos, L. Bacakova, B. Discher, F.S. Bates, D.E. Discher, Polymer vesicles in vivo: correlations with PEG molecular weight, J. Control. Release 90 (2003) 323–334.
[24] T. Kawano, T. Okuda, H. Aoyagi, T. Niidome, Long circulation of intravenously administered plasmid DNA delivered with dendritic poly(L-lysine) in the blood flow, J. Control. Release 99 (2004) 329–337.
[25] B. Romberg, W.E. Hennink, G. Storm, Sheddable coatings for long-circulating nanoparticles, Pharm. Res. 25 (2008) 55–71.
[26] T. Safra, F. Muggia, S. Jeffers, D.D. Tsao-Wei, S. Groshen, O. Lyass, R. Henderson, G. Berry, A. Gabizon, Pegylated liposomal doxorubicin (doxil): reduced clinical cardiotoxicity in patients reaching or exceeding cumulative doses of 500 mg/m^2, Ann. Oncol. 11 (2000) 1029–1033.
[27] S.E. Krown, D.W. Northfelt, D. Osoba, J.S. Stewart, Use of liposomal anthracyclines in Kaposi's sarcoma, Semin. Oncol. 31 (2004) 36–52.
[28] T.M. Allen, D.R. Mumbengegwi, G.J. Charrois, Anti-CD19-targeted liposomal doxorubicin improves the therapeutic efficacy in murine B-cell lymphoma and ameliorates the toxicity of liposomes with varying drug release rates, Clin. Cancer Res. 11 (2005) 3567–3573.
[29] F. Pastorino, D.R. Mumbengegwi, D. Ribatti, M. Ponzoni, T.M. Allen, Increase of therapeutic effects by treating melanoma with targeted combinations of c-myc antisense and doxorubicin, J. Control. Release 126 (2008) 85–94.
[30] T.A. ElBayoumi, V.P. Torchilin, Tumor-targeted nanomedicines: enhanced antitumor efficacy in vivo of doxorubicin-loaded, long-circulating liposomes modified with cancer-specific monoclonal antibody, Clin. Cancer Res. 15 (2009) 1973–1980.
[31] H. Shmeeda, L. Mak, D. Tzemach, P. Astrahan, M. Tarshish, A. Gabizon, Intracellular uptake and intracavitary targeting of folate-conjugated liposomes in a mouse lymphoma model with up-regulated folate receptors, Mol. Cancer Ther. 5 (2006) 818–824.
[32] A. Gabizon, A.T. Horowitz, D. Goren, D. Tzemach, H. Shmeeda, S. Zalipsky, In vivo fate of folate-targeted polyethylene-glycol liposomes in tumor-bearing mice, Clin. Cancer Res. 9 (2003) 6551–6559.
[33] R.M. Schiffelers, G.A. Koning, T.L. ten Hagen, M.H. Fens, A.J. Schraa, A.P. Janssen, R.J. Kok, G. Molema, G. Storm, Anti-tumor efficacy of tumor vasculature-targeted liposomal doxorubicin, J. Control. Release 91 (2003) 115–122.
[34] U.B. Nielsen, D.B. Kirpotin, E.M. Pickering, K. Hong, J.W. Park, M. Refaat Shalaby, Y. Shao, C.C. Benz, J.D. Marks, Therapeutic efficacy of anti-ErbB2 immunoliposomes targeted by a phage antibody selected for cellular endocytosis, Biochim. Biophys. Acta 1591 (2002) 109–118.
[35] T. Kobayashi, T. Ishida, Y. Okada, S. Ise, H. Harashima, H. Kiwada, Effect of transferrin receptor-targeted liposomal doxorubicin in P-glycoprotein-mediated drug resistant tumor cells, Int. J. Pharm. 329 (2007) 94–102.
[36] R. Suzuki, T. Takizawa, Y. Kuwata, M. Mutoh, N. Ishiguro, N. Utoguchi, A. Shinohara, M. Eriguchi, H. Yanagie, K. Maruyama, Effective anti-tumor activity of oxaliplatin encapsulated in transferrin-PEG-liposome, Int. J. Pharm. 346 (2008) 143–150.
[37] J.W. Park, K. Hong, D.B. Kirpotin, G. Colbern, R. Shalaby, J. Baselga, Y. Shao, U.B. Nielsen, J.D. Marks, D. Moore, D. Papahadjopoulos, C.C. Benz, Anti-HER2 immunoliposomes: enhanced efficacy attributable to targeted delivery, Clin. Cancer Res. 8 (2002) 1172–1181.
[38] R.E. Eliaz, F.C. Szoka, Liposome-encapsulated doxorubicin targeted to CD44: a strategy to kill CD44-overexpressing tumor cells, Cancer Res. 61 (2001) 2592–2601.
[39] Y. Lu, J. Yang, E. Sega, Issues related to targeted delivery of proteins and peptides, Aaps J. 8 (2006) E466–478.
[40] O. Tredan, C.M. Galmarini, K. Patel, I.F. Tannock, Drug resistance and the solid tumor microenvironment, J. Natl. Cancer Inst. 99 (2007) 1441–1454.
[41] J.L. Au, R.R. Kumar, D. Li, M.G. Wientjes, Kinetics of hallmark biochemical changes in paclitaxel-induced apoptosis, AAPS PharmSci 1 (1999) E8.
[42] J.L. Au, S.H. Jang, M.G. Wientjes, Clinical aspects of drug delivery to tumors, J. Control. Release 78 (2002) 81–95.

Evasion of the Accelerated Blood Clearance Phenomenon by Coating of Nanoparticles with Various Hydrophilic Polymers

Tsutomu Ishihara,*,†,‡ Taishi Maeda,† Haruka Sakamoto,† Naoko Takasaki,† Masao Shigyo,† Tatsuhiro Ishida,§ Hiroshi Kiwada,§ Yutaka Mizushima,|| and Tohru Mizushima†

Graduate School of Medical and Pharmaceutical Sciences, Kumamoto University, Kumamoto 862-0973, Japan, Department of Chemical Biology and Applied Chemistry, College of Engineering, Nihon University, Fukushima 963-8642, Japan, Institute of Health Bioscience, The University of Tokushima, Tokushima 770-8505, Japan, and DDS Institute, The Jikei University School of Medicine, Tokyo 105-8461, Japan

Received July 7, 2010; Revised Manuscript Received August 6, 2010

The accelerated blood clearance (ABC) phenomenon is induced upon repeated injections of poly(ethylene glycol) (PEG)-coated colloidal carriers. It is essential to suppress this phenomenon in a clinical setting because the pharmacokinetics must be reproducible. In this study, we evaluated the induction of the ABC phenomenon using nanoparticles coated with various hydrophilic polymers instead of PEG. Nanoparticles encapsulating prostaglandin E1 were prepared by the solvent diffusion method from a blend of poly(lactic acid) (PLA) and block copolymers consisting of various hydrophilic polymers and PLA. Coating of nanoparticles with poly(*N*-vinyl-2-pyrrolidone) (PVP), poly(4-acryloylmorpholine), or poly(*N*,*N*-dimethylacrylamide) led to extended residence of the nanoparticles in blood circulation in rats, although they had a shorter half-life than the PEG-coated nanoparticles. The ABC phenomenon was not induced upon repeated injection of PVP-coated nanoparticles at various time intervals, dosages, or frequencies, whereas it was elicited by PEG-coated nanoparticles. In addition, anti-PVP IgM antibody, which is estimated to be one of the crucial factors for induction of the ABC phenomenon, was not produced after injection of PVP-coated nanoparticles. These results suggest that the use of PVP, instead of PEG, as a coating material for colloidal carriers can evade the ABC phenomenon.

Introduction

During the last three decades, many studies have focused on "polymer therapeutics," in which pharmaceuticals are modified with synthetic polymers.[1] Poly(ethylene glycol) (PEG) has been widely used as a modifying material for proteins, peptides, aptamers, and various types of colloidal carriers.[2−4] The modification of pharmaceuticals with PEG chains leads to altered physicochemical characteristics (e.g., solubility and stability) as well as changes in immunogenicity, elimination, and cellular uptake. As a result, pegylated proteins and carriers remain in the blood circulation for a prolonged duration. Because long-circulating proteins have continuous and longer-term activity, some pegylated proteins have already been used in a clinical setting.[1,4] Long-circulating colloidal carriers (so-called "stealth carriers") show preferential accumulation in tumors and at sites of inflammation because of the enhanced permeability and retention (EPR) effect.[5] Considerable efforts have been made to develop various pegylated carriers such as liposomes, solid nanoparticles, and polymeric micelles for use as therapeutic agents for expanding the utility of drugs in clinical settings.[6−10] A pegylated liposome containing doxorubicin (Doxil/Caelyx) has been clinically used for the treatment of cancer, and many other types of pegylated carriers are currently undergoing clinical trials.

As synthetic polymers are expected to lead to the development of polymer therapeutics, some nonionic hydrophilic polymers have been proposed as PEG alternatives. Proteins and colloidal carriers have been covalently modified with poly(*N*-vinyl-2-pyrrolidone) (PVP),[11,12] poly(4-acryloylmorpholine) (PAcM),[11] poly(*N*,*N*-dimethylacrylamide) (PDMAA),[12] poly(acrylamide),[12] poly(vinyl alcohol) (PVA),[12,13] poly(oxazoline),[14] poly(amino acids),[15] poly(glycerol),[16] and poly(*N*-2-hydroxypropyl methacrylamide)[17,18] resulting in extended residence in the circulation. In the majority of cases, however, their distinct advantages over PEG have not yet been verified.

One pharmacokinetic issue for pegylated liposomes, the so-called accelerated blood clearance (ABC) phenomenon, has come to the forefront.[19,20] In this phenomenon, a second dose of pegylated liposomes is rapidly cleared from the circulation when administered within a certain time interval from administration of the first dose on account of accelerated accumulation of these liposomes in the liver. The ABC phenomenon is of clinical concern because it decreases the therapeutic efficacy of an encapsulated drug upon repeated administration and may cause adverse effects because of altered biodistribution of the drug. The time interval between repeated injections, dose and physicochemical properties of the pegylated liposomes, and the species of the encapsulated drugs have been shown to affect the extent of the ABC phenomenon.[21−25] Although the mechanism governing the ABC phenomenon is still unclear, it was proposed that this phenomenon involves sequential events, including induction of anti-PEG IgM antibody production in the spleen by the first dose of pegylated liposomes, complement activation by the IgM antibody, and opsonization by C3 fragments following the second dose of pegylated liposomes

* To whom correspondence should be addressed. Phone and Fax: +81-24-956-8805. E-mail: ishihara@chem.ce.nihon-u.ac.jp.
† Kumamoto University.
‡ Nihon University.
§ The University of Tokushima.
|| The Jikei University School of Medicine.

10.1021/bm100754e
Published on Web 08/26/2010

and their uptake by the mononuclear phagocyte system (MPS).[21,26] The ABC phenomenon was also observed using pegylated polymeric micelles[27] and nanoparticles.[28]

Several approaches have been proposed for the suppression of the ABC phenomenon, including changes in the physicochemical properties of pegylated carriers[22,27,29] and changes in the administration regimen such as injection dose or time interval between doses.[22,29,30]

Another approach is to replace PEG with a new polymer that does not induce the ABC phenomenon. Romberg et al. reported that liposomes coated with poly(hydroxyethyl L-glutamine) or poly(hydroxyethyl L-asparagine) showed similar stealth properties and reduced ABC compared to PEG-coated liposomes.[31] However, the ABC phenomenon was still elicited when those liposomes were injected at low doses.

In previous reports, we described the preparation of polymeric nanoparticles from a blend of poly(lactic acid) (PLA) homopolymers and PEG-poly(lactide) (PEG-PLA) block copolymers by the solvent diffusion method.[32,33] The drugs prostaglandin E1 (PGE_1) and betamethasone disodium phosphate could be efficiently encapsulated in the nanoparticles by a unique technique involving the use of a metal.[32,34] The nanoparticles showed extended residence in the circulation, resulting in a preferential accumulation in the inflammatory lesion[35] and the vascular lesion[34] by the EPR effect. However, the nanoparticles elicited the ABC phenomenon.[29] In the present study, we prepared PGE_1-encapsulating nanoparticles from a mixture of PLA homopolymer and block copolymers consisting of PLA and various hydrophilic polymers (PVP, PAcM, PDMAA, and PVA; Supporting Information, Figure 1) and examined whether these nanoparticles induced the ABC phenomenon.

Experimental Section

1. Materials and Animals. Poly(L-lactic acid) (L-PLA) and poly(D,L-lactic acid) (D,L-PLA) were supplied from Taki Chemical Co., Ltd. (Kakogawa, Japan). PGE_1 was purchased from Cayman Chemical Co. (Ann Arbor, MI). Iron chloride and *N*-vinyl-2-pyrrolidone were purchased from Wako Pure Chemicals Industries, Ltd. (Osaka, Japan). 4-Acryloylmorpholine and *N*,*N*-dimethylacrylamide were purchased from Tokyo Chemical Industry Co., Ltd. (Tokyo, Japan).

Male Wistar rats (6 weeks old) were obtained from Kyudo Co., Ltd. (Kumamoto, Japan). The rats were allowed free access to water and rat chow and were housed under controlled environmental conditions (constant temperature, humidity, and a 12 h dark−light cycle). The experiments and procedures described herein were carried out in accordance with the Guide for the Care and Use of Laboratory Animals as adopted and promulgated by the National Institutes of Health and were approved by the Animal Care Committee of Kumamoto University.

2. Syntheses of Block Copolymers. PEG-PLA block copolymer was synthesized by ring-opening polymerization of D,L-lactide (Purac America, Lincolnshire, IL) in the presence of monomethoxy-PEG-hydroxyl (Nippon Oil and Fats Co., Tokyo, Japan) in accordance with the reported method.[36] PVP-PLA, PAcM-PLA, and PDMAA-PLA were synthesized by radical polymerization of a corresponding monomer in the presence of PLA with a terminal thiol group.[37] The polymerization of *N*-vinyl-2-pyrrolidone, 4-acryloylmorpholine, and *N*,*N*-dimethylacrylamide (1100 mg each) was carried out in dimethylformamide (DMF; 1 mL) in the presence of an initiator, azobisisobutyronitrile (AIBN; 10 mg), for 4 h at 70 °C under an argon atmosphere. To prepare block copolymers with PLA, PLA with a terminal thiol group (300 mg) was added to the system as a chain transfer agent. The resulting polymers were dissolved in 5 mL of acetonitrile, and the solution was slowly added to 500 mL of water to form colloidal particles of block copolymers. To purify the block copolymers, the aqueous suspension was filtered twice using a Minimate TFF capsule with a 300 kDa Omega membrane (Pall Co., Port Washington, NY). The suspension was concentrated using a Centriprep centrifugal filter device with an Ultracel 50 kDa membrane (YM-50; Millipore Co., Billerica, MA), and the polymers were finally obtained by lyophilization. PVA with a terminal thiol group was supplied by Kuraray Co. (Tokyo, Japan). The degree of saponification of the polymer is shown as 87−89 mol % in the catalogue. PLA (300 mg) with a terminal pyridyl disulfide group and PVA (1200 mg) with a terminal thiol group were mixed in 10 mL of dimethyl sulfoxide (DMSO) for 12 h at room temperature. The resulting block copolymers were purified using a TFF capsule as mentioned above.

Supplied D,L-PLA has a carboxylic group at the end of the polymer chain, as shown in a previous report.[32] Thus, PLA with a thiol group was obtained by condensation of aminoethanethiol to PLA. D,L-PLA (2000 mg; M_w 18300; M_n 13500), diisopropyl-carbodiimide (234 mg), and 2-aminoethanethiol hydrochloride (210 mg) were mixed in 5 mL of DMSO for 12 h at room temperature. The resulting polymer was precipitated twice in an excess of 2-propanol. The precipitate of the polymer was dissolved in chloroform, and the solution was washed in water five times. After evaporation of chloroform, the polymer was dispersed in water and finally obtained by lyophilization. Determination of the carboxylic group content by 9-anthryldiazomethane[32] showed that 70% of the carboxylic groups of PLA were modified. PLA with a terminal pyridyl disulfide group was obtained by mixing PLA with a thiol group and excess 2−2′-dithiopyridine in DMSO for 2 h at room temperature. The modified PLA molecules were purified 3 times by precipitation in 2-propanol.

The molecular weights of methoxy-PEG-hydroxyl and PVA were determined by size-exclusion chromatography (SEC) on a TSK-GEL α-3000 column and a TSK-GEL α-2500 column (Tosoh Co., Tokyo, Japan) with a refractive index (RI) detector using 0.1 M $NaNO_3$ aqueous solution as the mobile phase. The instrument was calibrated with monodispersed PEG standards (Tosoh). The block polymers (PVP-PLA, PAcM-PLA, and PDMAA-PLA) were incubated in 2 N NaOH aqueous solution for 12 h at 40 °C to hydrolyze PLA. After neutralization of the solution by addition of HCl solution, the molecular weight of the hydrophilic homopolymer in the solution was determined by SEC as mentioned above. The molecular weights of PLA and PEG-PLA were determined by SEC on a Shodex KF803L column (Showa Denko, Tokyo, Japan) with an RI detector using THF as the mobile phase. The instrument was calibrated with monodispersed polystyrene standards (Tosoh).

The composition of the block copolymers was evaluated by ^1H NMR in chloroform-*d*. The composition was also calculated from the M_w values of a hydrophilic polymer segment and a PLA segment.

3. Preparation of Nanoparticles. Nanoparticles were prepared by the oil-in-water solvent diffusion method in the presence of iron as reported previously.[29,34] Block copolymers (25 mg), PGE_1 (10 mg), and diethanolamine (9.5 mg) were dissolved in 1050 μL of acetone, while L-PLA (25 mg; M_w 17500; M_n 15400) was dissolved in 450 μL of 1,4-dioxane. After mixing these solutions, 30 μL of 0.5 M iron(III) chloride anhydrous acetone solution was added. The resulting mixture was allowed to stand for 10 min at room temperature. The mixture was quickly added to 25 mL of distilled water with continuous stirring at 1000 rpm. A combination of 2.5 mL of 0.5 M citrate (pH 7.2) aqueous solution and 125 μL of 200 mg/mL polysorbate 80 aqueous solution was immediately added. The nanoparticles were purified using a Minimate TFF capsule with a 300 kDa Omega membrane (Pall) and condensed by a YM-50 (Millipore). Finally, the nanoparticles were sterilized by filtration through a 0.2-μm regenerated cellulose membrane (Minisart RC, Sartorius AG, Göettingen, Germany). To prepare nanoparticles from PVA-PLA, a mixture of 750 μL of DMSO, 450 μL of acetone, and 300 μL of 1,4-dioxane was used as a solvent to dissolve all compounds. Nanoparticles were also formed from L-PLA in the absence of block copolymers by the addition of 4 mL of acetone/dioxane (3/7 v/v) solution containing 50 mg of L-PLA (M_w 17500; M_n 15400), 9.5 mg diethanolamine, 10 mg PGE_1, and 35 μL of 0.5 M iron(III)

Table 1. Syntheses of Various Block Copolymers Consisting of a Hydrophilic Polymer and PLA

block copolymer	method	molecular weight of hydrophilic polymer[d]		hydrophlic polymer/block copolymer (wt %)[e]	
		M_w	M_n	^{1}H NMR	SEC
PEG-PLA	ring-opening polymerization[a]	5600	5400	54	ND[f]
PVP-PLA	radical polymerization[b]	35300	21400	71	66
PAcM-PLA	radical polymerization[b]	26700	14600	59	59
PDMAA-PLA	radical polymerization[b]	27800	16200	66	60
PVA-PLA	conjugation[c]	17000	12600	ND[f]	48

[a] D,L-Lactide was polymerized in the presence of methoxy-PEG-hydroxyl and stannous octoate. [b] The monomer (*N*-vinyl-2-pyrrolidone, 4-acryloylmorpholine, or *N,N*- dimethylacrylamide) was polymerized in DMF in the presence of AIBN and D,L-PLA (M_w 18300; M_n 13500) with a terminal thiol group. [c] Poly(vinyl alcohol) with a terminal thiol group was conjugated to D,L-PLA (M_w 18300; M_n 13500) with a pyridyl disulfide group via disulfide linkage. [d] Molecular weights of the hydrophilic polymers were determined by SEC. [e] The content of hydrophilic polymers in the block copolymers was calculated from the relative peak area of the ^{1}H NMR spectra of block copolymers and/or from the M_w values of each segment determined by SEC. [f] ND: not determined.

chloride anhydrous acetone solution to 25 mL of a 2% aqueous solution of polysorbate 80.

Particle size was determined by the dynamic light scatter method (Zetasizer Nano ZS, Malvern Instruments Ltd., Worcestershire, U.K.). The zeta potentials of the particles were also determined in 10 mM sodium phosphate buffer solution (pH 7.0) under a constant applied voltage (60 V). Each measurement of the same batch was carried out in triplicate. Nanoparticle weight was defined as the total PLA content in the nanoparticles. The PLA content and the loading efficiency of PGE_1 in nanoparticles were determined by a previously reported method.[34]

4. Animal Experiments. Various types of PGE_1-encapsulating nanoparticles suspended in saline were intravenously administered to rats via the tail vein at a dose of 50 or 1000 μg/rat. After designated intervals, the nanoparticles were administered again at a dose of 1000 μg/rat. At the indicated time, blood was collected from the tail vein using heparin-treated capillary tubes, and the blood concentration profile of PGE_1 was then determined using a PGE_1 EIA Kit (R&D Systems Inc., Minneapolis, MN) as described previously.[29,34] In brief, 50 μL of each blood sample was mixed with 400 μL of 1,4-dioxane and 50 μL of 10 mM EDTA (pH 7.0) to extract PGE_1 from the nanoparticles. After centrifuging this mixture at 13400 × *g* for 10 min, the supernatant (200 μL) was evaporated to dryness and dissolved in 500 μL of the immunoassay buffer supplied with the kit. The obtained solution was used for the immunoassay. The AUC from 0 to 24 h postinjection and blood clearance (CL) were calculated using the trapezoidal method.

5. Determination of IgM Antibody in Plasma. Qualification of IgM antibody in plasma was determined by the enzyme-linked immunosorbent assay (ELISA) as described previously[29] with minor modifications. The polymers were dissolved in 50 μL of organic solvent and added to 96-well plates (EIA/RIA Plates, AGC Techno Glass Co., Ltd., Funabashi, Japan); they were dried by evacuation for 30 min at 50 °C. PEG-PLA in ethanol/acetonitrile (8/2 v/v), PVP-PLA in ethanol/acetonitrile (8/2 v/v), and L-PLA in acetonitrile were used as coating polymers. Next, 200 μL of blocking buffer (50 mM Tris/HCl [pH 8.0], 0.14 M NaCl, and 1% bovine serum albumin [BSA]) was added and incubated for 1 h, and the wells were washed three times with washing buffer (50 mM Tris/HCl [pH 8.0], 0.14 M NaCl, and 0.05% polysorbate 20). Plasma was obtained by centrifugation (15 min at 2700 × *g*) of collected blood samples and was diluted 25-fold with a dilution buffer (50 mM Tris/HCl [pH 8.0], 0.14 M NaCl, 1% BSA, and 0.05% polysorbate 20). Then, 100 μL of the solution was added to the wells and incubated for 1 h. The wells were washed five times with washing buffer, and 100 μL of horseradish peroxidase (HRP)-conjugated antibody (0.2 μg/mL, goat antirat IgM IgG-HRP conjugate; Bethyl Laboratories, Inc., Montgomery, TX) in dilution buffer was added to each well. After incubation for 1 h, the wells were again washed five times with washing buffer. Coloration was initiated by the addition of *o*-phenylene diamine (1 mg/mL; Sigma, St. Louis, MO) and hydrogen peroxide and was stopped by addition of 100 μL of 2 M H_2SO_4 aqueous solution. The absorbance was measured at 490 nm using a microplate reader.

Table 2. Properties of Nanoparticles Prepared from Block Copolymers

code	block copolymer	diameter[a] (nm) [PDI[b]]	zeta potential[a] (mV)	PGE_1 loading efficiency (%)
PEG-NP	PEG-PLA	133 ± 8 [0.12]	−1.3 ± 0.9	1.05
PVP-NP	PVP-PLA	122 ± 10 [0.15]	−3.0 ± 0.6	0.67
PAcM-NP	PAcM-PLA	125 ± 4 [0.16]	−2.7 ± 0.7	1.01
PDMAA-NP	PDMAA-PLA	131 ± 2 [0.18]	−2.6 ± 0.4	0.81
PVA-NP	PVA-PLA	112 ± 4 [0.14]	−4.0 ± 0.7	0.37
NC-NP	none	118 ± 18 [0.15]	−14.5 ± 1.9	0.66

[a] The mean (SD) was calculated (n = 3). [b] PDI: polydispersity index.

Results

Block copolymers were synthesized by various methods (Table 1). PEG-PLA was synthesized by ring-opening polymerization of lactide in the presence of methoxy-PEG-hydroxyl according to the conventional method.[36] In the cases of PVP, PAcM, and PDMAA, the block polymers were synthesized by radical polymerization of the corresponding monomers in the presence of PLA with a functional thiol at its end, which was as a chain transfer agent. The resulting block copolymers were successfully purified from monomers and water-soluble polymers using ultrafiltration because block copolymers form small colloids in water. The M_w values of the PVP, PAcM, and PDMAA segments in the block copolymers were determined to be approximately 30000 by SEC (Table 1), and the M_w of the PLA segment was 18300. In general, PVA is synthesized by partial hydrolysis of poly(vinyl acetate) through alkali-hydrolysis (saponification). Although it may be possible to obtain poly(vinyl acetate)-PLA block copolymers by radical polymerization, as mentioned above, subsequent saponification also leads to hydrolysis of the PLA segment. Thus, we prepared PVA-PLA by conjugating PVA and PLA via a disulfide linkage. The content of hydrophilic polymers in the block copolymers was calculated from the relative peak areas of the ^{1}H NMR spectra of block copolymers and from the M_w values of each segment. As shown in Table 1, these values were almost coincident.

The nanoparticles encapsulating PGE_1 were similarly prepared from the block copolymers and PLA homopolymer according to the solvent diffusion method. The diameters of the resulting nanoparticles were approximately 120 nm (Table 2). The zeta potentials of the nanoparticles (PEG-, PVP-, PAcM-, PDMAA-, and PVA-NP) showed neutral values compared with those of noncoated nanoparticles (NC-NP) prepared from PLA alone without block copolymers, suggesting that the nanoparticle surfaces were coated with the corresponding hydrophilic polymers. The loading efficiency of PGE_1 in the nanoparticles was slightly less than 1% by weight except in the case of PVA-NP. The required use of DMSO to dissolve PVA-PLA in the

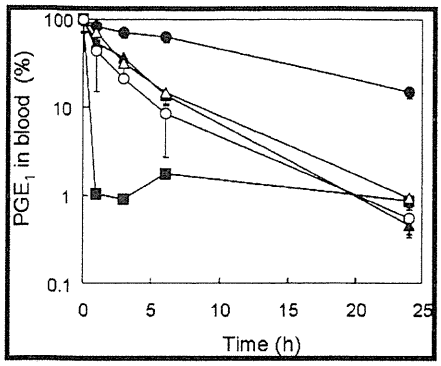

Figure 1. Blood clearance of nanoparticles in rats. Various nanoparticles encapsulating PGE_1, as shown in Table 2 (closed circle, PEG-NP; open circle, PVP-NP; closed triangle, PAcM-NP; open triangle, PDMAA-NP; closed square, PVA-NP), were injected intravenously at a dose of 1000 μg/rat, and the concentrations of PGE_1 in the blood were followed up to 24 h. Each data point represents the mean (SD) of three rats.

PVA-NP preparation, might have induced the lower encapsulation percentage.

In this study, the PGE_1 concentration in the blood was considered the concentration of nanoparticles for the following reasons. First, it has been reported that PGE_1 circulating in blood is rapidly metabolized during its passage through the lung.[38] A previous study using ^{3}H-labeled PGE_1 revealed that PGE_1 was metabolized to 13,14-dihydro-15-keto-PGE_1 and that only approximately 1.9% of the injected dose of PGE_1 remained intact in the plasma at 20 s after administration.[39] The results of our study are in agreement with these results in that PGE_1 could not be detected by an enzyme immunoassay performed at 5 min after PGE_1 administration.[34] Thus, it is suggested that the PGE_1 molecules in the nanoparticles but not the free (released) PGE_1 molecules were preferentially detected in the blood after the nanoparticle injection. Second, in this study, when the nanoparticles were incubated in vitro in diluted serum at 37 °C for at least 24 h, PGE_1 release from the nanoparticles was hardly detected. This result suggests that, in vivo, most PGE_1 molecules remain in the nanoparticles for 24 h. Taken together, the concentrations of PGE_1 in blood can be considered the concentration of the nanoparticles.

The nanoparticles shown in Table 2 were administrated to rats via the tail vein, and the PGE_1 concentrations in blood were monitored for 24 h. The NC-NP formed from PLA alone immediately cleared from the circulation because of MPS uptake, and the free PGE_1 was immediately cleared by metabolism.[34] The CL values of free PGE_1 and NC-NP were >2000 and 1880 mL/h/kg, respectively. In contrast, all nanoparticles except PVA-NP could retain PGE_1 for a prolonged time in the circulation (Figure 1). The CL values of PEG-NP, PVP-NP, PAcM-NP, and PDMAA-NP were 3.7, 25.7, 19.0, and 14.1 mL/h/kg, respectively. These nanoparticles can therefore be said to possess stealthiness, although the stealthiness of PVP-NP, PAcM-NP, and PDMAA-NP was significantly lower than that of PEG-NP. PVA-NP did not show prolonged residence in the blood, although the liposomes coated with PVA possessed stealthiness.[13] This may be because of the loss of flexibility of the PVA chains by the interactions of PVA with the surfaces of the nanoparticles.

We then evaluated whether PVP-NP and PEG-NP induced the ABC phenomenon. The dose of nanoparticles at the first injection was set at 50 or 1000 μg per rat, and the dose at the second injection was fixed at 1000 μg per rat because that amount was needed to detect PGE_1 in blood. The intervals

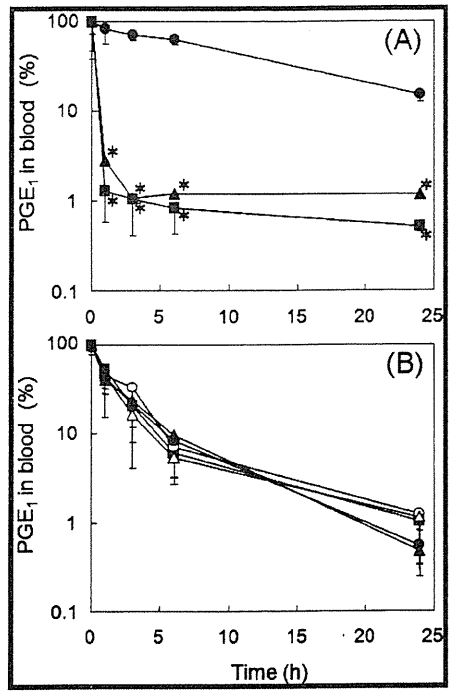

Figure 2. Induction of the ABC phenomenon upon injections of PEG-NP and PVP-NP. (A) Rats were pretreated with PEG-NP at a dose of 50 μg (square) or 1000 μg (triangle) per rat. At 7 d after the first injection, PEG-NP (1000 μg/rat) was injected again, and the concentration of PGE_1 in blood was followed up to 24 h. The clearance profile of PEG-NP at single administration (1000 μg/rat) is also shown (circle). (B) Rats were pretreated with PVP-NP at a dose of 50 μg/rat. At 3 (open circle), 7 (closed square), or 14 (open triangle) d after the first injection, PVP-NP (1000 μg/rat) was injected again. Alternatively, at 7 d after preinjection of PVP-NP (1000 μg/rat), PVP-NP (1000 μg/rat) was injected again (closed triangle). After the second injection, the concentration of PGE_1 in the blood was followed up to 24 h. The clearance profile of PVP-NP at single administration (1000 μg/rat) is also shown (closed circle). Each data point represents the mean (SD) of three rats. The asterisks indicate values that significantly differ from those measured for the corresponding nanoparticles upon single administration ($p < 0.05$).

between first and second injections were varied at 3, 7, or 14 d. PEG-NP apparently elicited the ABC phenomenon when PEG-NP (50 and 1000 μg) was injected 7 d in advance (Figure 2A). As described previously, the extent of the ABC phenomenon was the highest for the 7 d interval.[29] On the other hand, PVP-NP did not induce the ABC phenomenon when 50 μg of PVP-NP was injected 3, 7, or 14 d in advance of the second injection, nor when 1000 μg of PVP-NP was injected 7 d before the second injection (Figure 2B). PAcM-NP and PDMAA-NP also did not induce the ABC phenomenon when these nanoparticles were injected at a dose of 50 μg per rat 7 d before the second injection (1000 μg/rat; Figure 3).

Next, the rats were injected with the nanoparticles (50 or 1000 μg/rat) three times at 7 d intervals. At 7 d after the third injection, the same type of nanoparticle (1000 μg/rat) was injected to determine the time course of the PGE_1 concentration in blood. The rats that were pretreated with 50 μg of PEG-NP three times in advance showed rapid PGE_1 clearance (Figure 4A). Further, the rats pretreated with 1000 μg of PEG-NP showed the ABC phenomenon to a lesser extent (Figure 4A). This may be because high-dose administration of PEG-NP induced immunotolerance, as observed by high-dose administration of liposomes.[21] On the other hand, PVP-NP did not induce the ABC phenomenon after multiple injections of 50 and 1000 μg (Figure 4B).

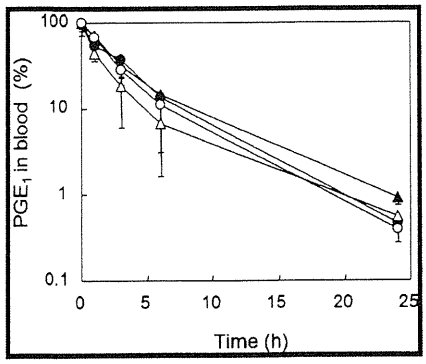

Figure 3. Induction of the ABC phenomenon upon injections of PDMAA-NP and PAcM-NP. Rats were pretreated with PDMAA-NP (open circle) and PAcM-NP (open triangle) at a dose of 50 μg/rat. At 7 d after the first injection, the same type of nanoparticle (1000 μg/rat) was injected again, and the concentrations of PGE_1 in blood were followed up to 24 h. The clearance profile of PDMAA-NP (closed circle) and PAcM-NP (closed triangle) at a single administration (1000 μg/rat) are also shown. Each data point represents the mean (SD) of three rats.

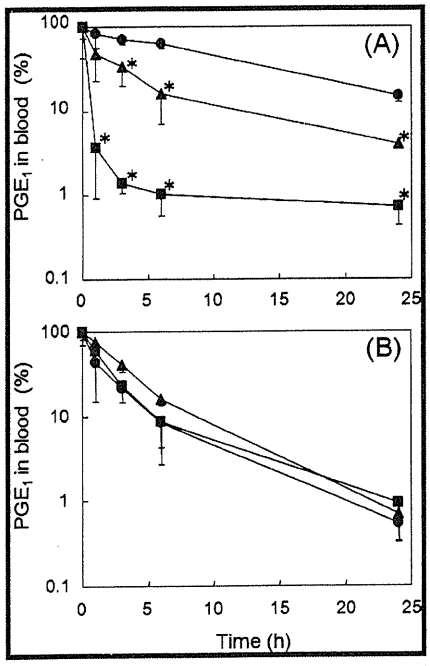

Figure 4. Induction of the ABC phenomenon upon multiple injections of nanoparticles. Rats were pretreated three times with (A) PEG-NP or (B) PVP-NP at a dose of 50 μg/rat (square) or 1000 μg/rat (triangle) every 7 d. At 7 d after the third injection, the same type of nanoparticle (1000 μg/rat) was injected to determine the concentration time course of PGE_1 in the blood. The clearance profiles of the nanoparticles at single administration (1000 μg/rat) are also shown (circle). Each data point represents the mean (SD) of three rats. The asterisks indicate values that significantly differ from those measured for the corresponding nanoparticles upon single administration ($p < 0.05$).

Induction of the ABC phenomenon was evaluated when the different types of nanoparticles were used at the first and second administrations (Figure 5). PEG-NP (50 μg/rat) was injected in advance, PVP-NP (1000 μg/rat) was injected 7 d later, and the concentration of PGE_1 in the blood was monitored. Alternatively, PEG-NP and PVP-NP were used in reverse order. PEG-NP did not induce the ABC phenomenon when PVP-NP was injected in advance. Moreover, PVP-NP did not induce the ABC phenomenon when PEG-NP was injected in advance.

Finally, we evaluated IgM production after nanoparticle administration. The IgM level was measured by ELISA using

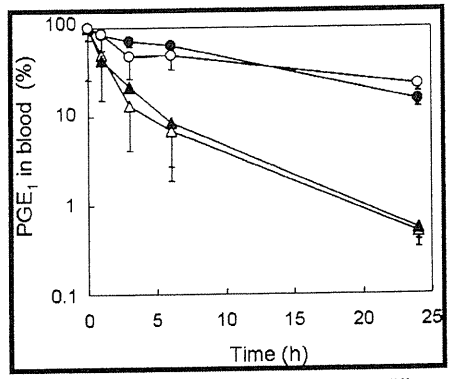

Figure 5. Induction of the ABC phenomenon by different types of nanoparticles. Rats were pretreated with PEG-NP at a dose of 50 μg/rat. After 7 d, PVP-NP (1000 μg/rat) was injected to follow the concentration of PGE_1 in the blood (open triangle). Alternatively, rats were pretreated with PVP-NP at a dose of 50 μg/rat, and then PEG-NP (1000 μg/rat) was injected after 7 d (open circle). The clearance profiles of PEG-NP (closed circle) and PVP-NP (closed triangle) upon single administration (1000 μg/rat) are also shown. Each data point represents the mean (SD) of three rats.

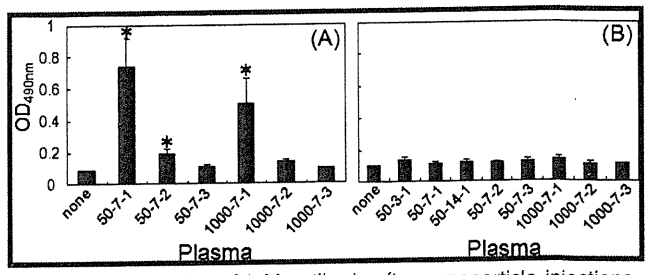

Figure 6. Production of IgM antibody after nanoparticle injections. (A) IgM in plasma collected from rats administered PEG-NP was detected by ELISA using a PEG-PLA-coated well. (B) IgM in plasma collected from rats administered PVP-NP was detected by ELISA using a PVP-PLA-coated well. Plasma was collected at various doses, intervals, and frequencies, and each plasma sample is annotated as follows: (dose of nanoparticles; μg/rat) − (time interval until collection or next injection; *d*) − (number of repetitions of injections). Absorbance from plasma of untreated rats is indicated as none. Each data point represents the mean (SD) of three rats. The asterisks indicate values that significantly differ from those measured as none ($p < 0.05$).

wells coated with polymers (PEG-PLA, PVP-PLA, and PLA; Supporting Information, Figure 2). IgM in the plasma of rats treated with PEG-NP was detected at a high level on the PEG-PLA-coated wells, but it was detected at much lower levels on the PVP-PLA-coated or PLA-coated wells. On the other hand, IgM in the plasma of rats treated with PVP-NP and in the plasma of untreated rats was not detected at all on any of the wells. Because the IgM level was not drastically affected by the PEG-PLA content used for coating in the range of 1.6−50.0 μg/well, the polymer content for coating was fixed at 12.5 μg/well. Based on these preliminary experiments, the IgM level in the plasma of rats that were administered PEG-NP and PVP-NP was analyzed on the wells coated with PEG-PLA and PVP-PLA, respectively. As shown in Figure 6, no anti-PVP IgM was detected in plasma from rats injected with PVP-NP, while anti-PEG IgM was detected at significant levels in those injected with PEG-NP.

Discussion

The ABC phenomenon is a crucial issue in the development of novel colloidal carriers because its pharmacokinetics must be reproducible in a clinical setting to prevent unanticipated